Link between the enzymatic kinetics and mechanical behavior in an actomyosin motor

メタデータ	言語: eng
	出版者:
	公開日: 2017-10-03
	キーワード (Ja):
	キーワード (En):
	作成者:
	メールアドレス:
	所属:
URL	http://hdl.handle.net/2297/7443

Link between the Enzymatic Kinetics and Mechanical Behavior in an Actomyosin Motor

Ichiro Amitani, Takeshi Sakamoto, and Toshio Ando

Department of Physics, Faculty of Science, Kanazawa University, Kanazawa 920-1192, Japan

ABSTRACT   We have attempted to link the solution actomyosin ATPase with the mechanical properties of in vitro actin filament sliding over heavy meromyosin. To accomplish this we perturbed the system by altering the substrate with various NTPs and divalent cations, and by altering ionic strength. A wide variety of enzymatic and mechanical measurements were made under very similar solution conditions. Excellent correlations between the mechanical and enzymatic quantities were revealed. Analysis of these correlations based on a force-balance model led us to two fundamental equations, which can be described approximately as follows: the maximum sliding velocity is proportional to $\sqrt{V_{max}K_m^A}$, where K_m^A is the actin concentration at which the substrate turnover rate is half of its maximum (V_{max}). The active force generated by a cross-bridge under no external load or under a small external load is proportional to $\sqrt{V_{max}/K_m^A}$. The equations successfully accounted for the correlations observed in the present study and observations in other laboratories.

INTRODUCTION

Cyclic interactions of myosin heads with actin coupled to ATP hydrolysis are the molecular basis of muscle contraction, cytokinesis, certain types of vesicle transport, and so forth. Several types of muscles contain myosin heavy and light chains characteristic of each type. They differ in the speed of unloaded shortening and in the magnitude of isometric tension. Even in a specific type of muscle these mechanical outputs vary depending on conditions. Non-muscle myosins and actins also exhibit distinct rates of movement. How does the actomyosin ATPase kinetics determine the mechanical performance of this molecular motor? One approach to this issue is to isolate myosins from various sources, and then compare the kinetics of actin-activated ATPase reaction of these myosins and their mechanical performance. This approach was pioneered by Bárány (1967) with myosins isolated from various muscles having known maximum speeds of shortening. He found that the ATPase activity was proportional to the speed of shortening of the parent muscles. Qualitatively similar correlations have been observed also by other groups with different mammalian smooth muscles (Malmqvist and Arner, 1991; Helper et al., 1988), frog skeletal muscle fibers with different myosin heavy chain composition (Edman et al., 1988), crab muscle fibers of different types (Galler and Rathmayer, 1992), and rabbit aorta and small arterial muscles containing myosin heavy chains differing at the NH_2-

termini (DiSanto et al., 1997). Another approach is to substitute various ATP analogs (NTPs) for ATP, using a given type of myosin. This approach was initiated by Blum (1955). Myosin can use a wide variety of NTPs as the energy source for the motile activity. Hasselbach (1956) reported an excellent correlation between the rate of NTP hydrolysis by actomyosin and the isometric tension of glycerinated muscle fibers. More recently, this study has been refined by several groups. It has been recognized that various NTPs have different affinities for actomyosin, and myosins complexed with these NTPs or their products have different affinities for actin (Pate et al., 1993; White et al., 1993). This was not carefully considered in the previous study by Hasselbach. Moreover, accumulation of the NTP hydrolysis products in fibers without an NTP-regeneration system must have reduced the tension. Therefore, the excellent correlation observed in 1956 has to be reexamined. Recent studies have shown that the isometric tension and unloaded shortening speed of skinned fibers in various NTPs have only moderate correlation with the acto-HMM or acto-S1 NTPase activities (Pate et al., 1993; Regnier et al., 1998). We note, however, that measurements of the mechanical properties and the chemical kinetics have not been made under similar conditions. For technical reasons, it is often so in studies with muscle fibers, where the mechanical measurements are made at higher ionic strength, while the measurements of solution chemical kinetics are made at low ionic strength. Moreover, the solution and fiber enzymatic activities have been measured in limited concentrations of NTPs.

Sheetz and Spudich (1983) developed a motility assay wherein myosin-coated particles move along parallel tracks of *Nitella* actin bundles. After the success of fluorescence microscopy in visualizing fluorescently labeled single actin filaments (Yanagida et al., 1984), a more versatile and stable assay was developed wherein actin filaments move over surfaces coated with myosin filaments (Kron and Spudich, 1986), or proteolytic fragments of myosin (Toyoshima

et al., 1987). These developments allow us to investigate actomyosin motility under wide varieties of solution conditions with myosins and actins from diverse species and cell types. It has now become possible to investigate the fundamental question regarding the mechanochemical coupling of the actomyosin motor mentioned above in greater detail. First, it has been shown that the velocity of actin filaments sliding over myosin-coated surfaces and the velocity of myosin-coated beads along actin cables is analogous (with slight differences, depending on conditions) to the speed of unloaded shortening of muscle fibers (Sheetz et al., 1984; Homsher et al., 1992). Despite this analogy, many previous studies have reported no direct correlation between the steady-state actin-activated MgATPase activity of myosin and the rate of movement in the in vitro motility assays. However, we have to be careful in interpreting these results because identical, or very similar, solution conditions have not always been used in the motility and enzymatic assays.

Having this caution in mind, let us briefly review several types of previous studies where rates of movement measured in the in vitro motility assays have been compared with the corresponding actin-activated substrate turnover rates in solution. 1) Dependence on myosin species: beads coated with myosin from skeletal muscle and *Dictyostelium* move on actin cables from *Nitella* at distinct velocities, and these velocities are proportional to the respective actin-activated ATPase activities (Sheetz et al., 1984). Phosphorylated platelet myosin and phosphorylated turkey gizzard myosin have similar actin-activated ATPase activities, yet show very dissimilar rates of movement in the *Nitella*-based assay (Umemoto et al., 1989). Skeletal muscle myosin light chain isoforms have the same maximum actin-activated ATPase activity, yet again they translocate actin filaments at distinct velocities (Lowey et al., 1993). Chimera myosins, constructed from *Dictyostelium* myosin by substituting the 50K/20K junction region with those from other species of myosins, exhibit actin-activated ATPase activities characteristic of the activity of the myosins from which the junction region was donated. The velocities of actin sliding propelled by these chimeras, on the contrary, have no correlation with those driven by the donor myosins (Uyeda et al., 1994). Similarly, no correlation has been found with myosins from other sources (Vale et al., 1984; Higashi-Fujime, 1991). However, we have to be cautious about interpreting these observations, because in most cases actin-activated ATPase activity has been measured at one concentration of actin (Note that Bárány also used one concentration of actin in his 1967 study), and also because the *Nitella*-based assay tends to show slower motility than the sliding actin filament assay, depending on the myosin type used (Wolenski et al., 1993). Chimeric heavy meromyosins, which are produced by substituting the 50K/20K loop of smooth muscle heavy meromyosin with that from skeletal or β-cardiac myosin, lose regulation by regulatory light chain phosphorylation. The chimeras and the wild type,

however, show moderate correlation of the motile activity observed in the sliding actin filament assay with the maximum acto-HMM ATPase activity and with the K_m for actin (Rovner et al., 1995). Tryptic cleavage of the 25K/50K loop of skeletal myosin inhibits its motor function without any significant changes in the enzymatic properties of actomyosin, while cleavage of the 50K/20K loop increases the K_m for actin without significant effect on the motor function (Bobkov et al., 1996). The rate constant for dissociation of ADP from various muscle myosins complexed with actin has been compared with the maximum shortening speed of the parent fibers (Siemankowski et al., 1985). These quantities show a strong correlation, although it is still open to question whether the state formed by adding ADP to actomyosin is on the ATP hydrolysis pathway (Sleep and Hutton, 1980). Contrary to this observation, a chimeric myosin containing the *Dictyostelium* myosin heavy chain with the 25K/50K loop from skeletal myosin propels actin filaments at a velocity slightly slower than the wild type, while the rate of mant-ADP release from the actin-chimera myosin S1 is more than two times larger than that from the actin-wild-type myosin S1 (Murphy and Spudich, 1998) (the affinities of mant-ADP and ADP binding to actin-S1 are similar). 2) Dependence on ATP analogs: the velocity of actin filament translocation has been examined by Shimizu et al. (1991) using 15 ATP analogs. The relative velocities do not correlate well with the actin-activated substrate turnover rates. The actin-activated substrate turnover rate varies in a relatively small range compared to the variation in the velocity of actin translocation. A similar study has been made using naturally occurring nucleotides by another group (Higashi-Fujime and Hozumi, 1996). Again, no correlation is found. In these studies, however, one concentration of actin and one concentration of substrate have been used in the measurements of the enzymatic activities. However, in similar studies a moderate correlation is found between the motile activity and the maximum substrate turnover rate (Pate et al., 1993; Regnier et al., 1998). In these studies the actin concentration is varied, but one concentration of substrate is used in the measurements of the substrate turnover rate. 3) Dependence on actin species: the maximum MgATPase activity of skeletal muscle myosin activated with yeast actin is significantly lower than with skeletal muscle actin, whereas the apparent K_m for yeast actin of myosin heads is slightly larger than for skeletal actin (Cook et al., 1993). Nevertheless, the sliding velocities of both actins are quite similar, while force production of skeletal muscle heavy meromyosin with yeast actin is lower than with skeletal muscle actin (Cook et al., 1993; Kim et al., 1996; Miller et al., 1996). Subtilisin cleavage of skeletal muscle actin at Met-47 and Gly-48 markedly increases the K_m for actin of myosin heads without changing the maximum ATP turnover rate. The sliding velocity of the cleaved actin filaments is slower than that of intact actin filaments (Schwyter et al., 1990). In contrast to the effect of subtilisin cleavage of actin

on the actin-activated ATPase of myosin, replacement by mutagenesis of aspartic acid residues of *Dictyostelium* actin with histidine residues reduces the maximum ATP turnover rate with moderate reduction in the K_m for actin. This replacement also reduces the sliding velocity of actin filaments (Sutoh et al., 1991). Actins modified at Cys-374 by different fluorophores have parallel effects on the velocity of actin sliding over HMM, the maximum actin-activated S1 ATPase activity, and the affinity of actin for S1 in ATP (Crosbie et al., 1994). 4) Dependence on other factors: binding of tropomyosin to actin has a parallel enhancement effect on the actomyosin ATPase activity and the rate of movement (Umemoto et al., 1989; Umemoto and Sellers, 1990; Okagaki et al., 1991; Wang et al., 1993). This effect is ascribed to an increase in the maximum ATPase activity (Umemoto et al., 1989); the optimum pH is around pH 7.0 for the actomyosin ATPase activity (Stone and Prevost, 1973). For the motile activity, the optimum pH has been reported to be around pH 7.0 (Sheetz et al., 1984; Warshaw et al., 1990; Sugiura et al., 1992), or pH 8.5 (Homsher et al., 1992). In the former three studies the rate of movement at pH 8.5 is very much less than at pH 7.0. The cause of this discrepancy is unknown. We have to note, however, that parallel measurements of the pH effects on the ATPase and the motile activities have never been carried out under the identical or very similar solution conditions. Within a range of ionic strength where smooth movement of either actin filaments or myosin-coated beads is observed, the rate of movement increases with increasing ionic strength (Homsher et al., 1992; Umemoto and Sellers, 1990; Warshaw et al., 1990; Harada et al., 1987; Takiguchi et al., 1990; Saito et al., 1994; Vale and Oosawa, 1990). The speed of isotonic and unloaded shortening of skinned muscle fibers also increases with increasing ionic strength when the ionic strength is lower than 100 mM (Gulati and Podolsky, 1981; Arheden et al., 1988). Although an increase in ionic strength is known to reduce the affinity (particularly in the presence of ATP), of myosin heads for actin, a systematic comparison of the effect of ionic strength on the motile activity with that on the actomyosin ATPase activity has never been made.

As seen in recent many reports, the relationship between the rate of movement and the actomyosin ATPase kinetics does not seem as simple as first suggested by Bárány in 1967. Our present situation regarding this central issue of the actomyosin motor seems confused. In part, this confusion may be because the identical or very similar solution conditions have not been used for measurements of the motile and enzymatic activities. Discrepancy is often seen in the previous studies wherein the ATPase assay is performed in a solution whose ionic strength is a few times lower than the motility assay solution. If the affinities for myosin of the two actin species have a different dependence on ionic strength, the order of the affinities can be reversed by changing ionic strength. Thus, we would misconstrue the

relationship between the motile activity and the actin affinity for myosin. In the present study, care was taken in this respect. To examine the links between the motor function and the enzymatic reaction of actin-heavy meromyosin the system was perturbed by altering the substrate with various NTPs and divalent cations, and by altering ionic strength. It was also taken into account that various NTPs have different affinities for actomyosin, and that myosins complexed with these NTPs or their products have different affinities for actin. The experiments made with these precautions revealed an excellent correlation between the mechanical properties and the kinetics of substrate hydrolysis. Moreover, to account for these correlations we constructed a model based on an idea that the balance of a positive force and a velocity-dependent negative force determines the maximum velocity of movement. This idea was originally proposed by Huxley (1957). Equations derived from this model linked the chemical kinetics to the actin translocation velocity and the force generated without external load or under a small external load. The equations coincided with the experimentally revealed correlations in the present study, and also with observations from other studies.

MATERIALS AND METHODS

Preparation of proteins

Myosin and actin were prepared from rabbit skeletal muscle according to the methods of Tonomura et al. (1966) and Spudich and Watt (1971), respectively. HMM was obtained by chymotryptic digestion of freshly prepared (not glycerinated) myosin according to Weeds and Pope (1977). After centrifugal removal of the nondigested myosin and light meromyosin in a solution of low ionic strength, HMM was quickly frozen in liquid nitrogen and stored in liquid nitrogen. The molar concentration of HMM was estimated on the basis of $E_{280}^{1\%} = 7.0$ and a molecular weight of 3.5×10^5, with correction for the turbidity (1.93 times the 330 nm absorbance was subtracted from the 280 nm absorbance). The molar concentration of F-actin was estimated on the basis of $E_{290}^{1\%} = 6.5$ and a molecular weight of 4.2×10^4 (1.68 times the 330 nm absorbance was subtracted from the 290 nm absorbance to correct for turbidity artifacts).

Actin-activated HMM NTPase assays

In the measurements below the concentration of HMM was adjusted, depending on the actin concentrations, NTPs and divalent cations, so that hydrolyzed NTP at the last time point amounts to <15% of the initial amount of NTP. In the first set of experiments we used various NTPs to alter the enzymatic kinetics of acto-HMM. NTPs we used are ATP, CTP, TTP, UTP, ITP, and GTP. Actin was polymerized in a solution containing 100 mM KCl, 1 mM MgCl₂, 0.2 mM CaCl₂, 5 mM Tris-HCl (pH 8.0), and 0.2 mM ATP. To remove ATP from the actin sample, the polymerized actin was centrifuged at $150,000 \times g$ for 1 h. The resulting pellet was dispersed in Buffer A (25 mM KCl, 25 mM imidazole-HCl (pH 7.6), 2 mM MgCl₂, 0.2 mM CaCl₂) and dialyzed against the same buffer. HMM was mixed with various concentrations of F-actin in Buffer A. The NTPase reaction was initiated by the addition of NTP. The concentration of NTP was varied. In the second set of experiments we used various divalent cations as the complexing agents with ATP. Divalent cations we used are Mg²⁺, Mn²⁺, Ni²⁺, and Sr²⁺, all in the chloride form. Except for the case of Mg²⁺, actin pellet was dispersed in Buffer B (25 mM KCl, 25 mM

imidazole-HCl (pH 7.6), 0.2 mM $CaCl_2$) and dialyzed against Buffer B. The ATPase reaction was initiated by adding 2 mM ATP and 2 mM divalent cation together to a solution containing HMM and various concentrations of F-actin in Buffer B. In the third set of experiments actin-activated HMM MgATPase activity was measured in solutions of various ionic strengths. The solvents (Buffer C) contained various concentrations of KCl, 25 mM imidazole-HCl (pH 7.6), 2 mM $MgCl_2$, and 0.2 mM $CaCl_2$. The concentration of MgATP was 2 mM. When the acto-HMM MgATPase activities were measured at [ATP] < 0.2 mM, an ATP-regeneration system consisting of phosphoenol pyruvate, pyruvate kinase, NADH, and lactate dehydrogenase was used. The reaction was monitored by measuring the time course of the change in absorption of NADH at 340 nm. In all the other cases, amounts of phosphate liberated at 25°C were quantified by the method of Fiske and Subbarow (1925). The activities of HMM alone at each condition of substrate or ionic strength were subtracted from each determined activity of acto-HMM under the identical condition. The NT-Pase activities were determined by analyzing the amounts of phosphate liberated at six time points by the least-squares criterion. The absence of the perturbation effect of Mn^{2+}, Ni^{2+}, and Sr^{2+} upon the phosphate assay was confirmed.

Determination of kinetic parameters

At a given concentration of NTP the acto-HMM NTPase activity, V_{NTP}, was measured as above at seven different actin concentrations. The maximum activity (V_m^A) at infinite concentration of actin and the actin concentration, $K_{0.5}^A$, that gave the half maximum activity were determined, a simple hyperbolic dependence of V_{NTP} on actin concentration being assumed. The values of V_m^A and $K_{0.5}^A$ were obtained at six different concentrations of NTP. The maximum activity (V_{max}; see Table 1 for parameters) at infinite concentrations of actin and NTP, and the actin concentration, K_m^A ($K_{0.5}^A$ at infinite concentration of NTP), were determined, simple hyperbolic dependence of V_m^A and $K_{0.5}^A$ on MgNTP concentration being assumed. The MgNTP concentration, K_m^N, at which V_m^A is half of V_{max}, was determined from the relationship of V_m^A versus [MgNTP].

TABLE 1   List of parameters

d	Length of power stroke
$\langle f_s \rangle$	Magnitude of sliding force (active force) averaged over the substrate turnover time
$\langle f_r \rangle$	Time-averaged magnitude of resistive force
F_u	Force required to unbind a rigor head
Γ	Elastic constant of cross-bridge
k_{-w}	First-order dissociation rate constant of weakly bound cross-bridge
k_{+w}	Second-order binding rate constant in the weak-binding states
k_{+1}	Second-order rate constant of substrate binding to A · M
k_{+6}	Forward rate constant in the rate-limiting step (isomerization rate from A · M · ADP · Pi to A · M* · ADP · Pi)
K_m^A	Actin concentration for half-maximum NTPase rate
K_m^N	Substrate concentration for half-maximum NTPase rate
K_s^N	Substrate concentration for half-maximum sliding velocity
λ_w	Fraction of weakly bound cross-bridge
λ_{rig}	Fraction of rigor cross-bridge
p	Magnitude of power stroke (force spike)
ρ	Molar ratio of NEM-HMM over intact HMM
$[S]$	Substrate concentration
T_c	Substrate turnover time
T_p	Duration of power stroke
T_w	Lifetime of weakly bound cross-bridge
V_{max}	Maximum substrate turnover rate
V_s	Sliding velocity of actin filament
V_s^{max}	Maximum velocity of actin sliding

In vitro motility assay

Sliding filament in vitro motility assays were carried out as described in (Toyoshima et al., 1987) with some modifications. The temperature was maintained at 25°C for all assays. To pre-remove ATP-insensitive HMM, 5 μM HMM was mixed with 10 μM F-actin in a solution containing 0.1 M KCl, 3 mM $MgCl_2$, 0.2 mM $CaCl_2$, and 5 mM Tris-HCl (pH 8.0) at 25°C. The mixture was incubated for 20 min and then cooled to 0°C. After adding 2 mM ATP and 1 mM potassium pyrophosphate, the mixture was immediately centrifuged at 150,000 × g for 1 h. HMM in the supernatant was diluted to 0.3 μM with Buffer A, and then applied to a flow cell (~50 μl in volume) made of two coverslips (24 × 36 mm^2 and 22 × 22 mm^2), where the larger coverslip had been coated with nitrocellulose. The cell was incubated for 2 min. Unattached HMM was washed out by applying 50 μl of Buffer A from one side of the cell and by sucking, with a piece of filter paper, from the other side of the cell. This wash was repeated five times. BSA (1 mg/ml, 100 μl) dissolved in Buffer A was then applied to the cell, incubated for 2 min, and unattached BSA was washed either with Buffer A (when NTPs were the alterant), Buffer B (when divalent cations were the alterant), or Buffer C (when [KCl] was the alterant). Tetramethylrhodamine-phalloidine-labeled F-actin (2 nM, 100 μl) in the same buffer solution was applied to the cell and incubated for 30 s. The motion of actin filaments was initiated by applying 100 μl of a test solution that additionally contained oxygen-scavenging reagents (1% 2-mercaptoethanol, 4.5 mg/ml glucose, 0.216 mg/ml glucose-oxidase, 0.36 mg/ml catalase). When Ni^{2+} was used as a complexing agent with ATP, 2-mercaptoethanol was omitted from the oxygen-scavenging reagents. The test solution conditions were the same as those used for the actin-activated HMM NTPase assays. Both open sides of the flow cell were sealed with white Vaseline. The sliding motion of individual actin filaments was observed under an epiluminescence fluorescence microscope (Olympus IX70, Tokyo, Japan; equipped with an oil-immersion objective, 100×, NA 1.35), the images being taken with a SIT video camera (C2400-08, Hamamatsu Photonics, Shizuoka, Japan) and being recorded with a Hi8 video cassette recorder (EVO-9650, Sony, Tokyo, Japan). The recorded images were digitized with an image processor (Excel, Nippon Avionics, Osaka, Japan) and the two-dimensional coordinates of the rear end of each actin filament were chased frame by frame. Length of a track connecting these coordinates during a given period of time was calculated and averaged over >50 actin filaments. The sliding velocity was obtained by dividing the average value of the lengths of tracks by the given period of time.

In vitro motility assays with noncycling cross-bridges

Chemically damaged and therefore noncycling HMM was prepared by extensive treatment of HMM with NEM. HMM (30 μM) dialyzed against 30 mM KCl, 25 mM Tris-HCl (pH 8.0), and 0.1 mM PMSF was mixed with 9 mM NEM and incubated for 1 h at 25°C. The sample was cooled in an ice-water bath, mixed with 180 mM dithiothreitol, and dialyzed against a large volume of 25 mM KCl, 2 mM $MgCl_2$, 0.2 mM $CaCl_2$, 25 mM TES-KOH (pH 7.0), 1 mM 2-mercaptoethanol, and 0.1 mM PMSF. The modified sample was frozen in liquid nitrogen and stored in liquid nitrogen. Intact HMM pretreated for removing ATP-insensitive HMM heads was mixed with NEM-treated HMM at given ratios in either Buffer A, Buffer B, or Buffer C. The total concentration of intact and noncycling HMM was adjusted to 0.3 μM. The succeeding procedures were the same as those mentioned in the preceding subsection. Immediately after initiating the movement of actin filaments, the fluorescent images of actin filaments were recorded at five different surface areas. The recording time per one area was adjusted depending on the velocity of sliding actin filaments. When the velocity was relatively high, it was minimized to be 20 s. When the velocity was very low, it was ~2 min. After recording, ~40 actin filaments on one observation area were arbitrarily picked up for analysis of the average sliding velocity as a function of the molar ratio (ρ) of NEM-

HMM to intact HMM. The data were obtained from the five observation areas and then averaged.

Determination of the relative magnitude of sliding force

When actin filaments are sliding freely on HMM, the time-averaged active force generated by a cross-bridge must be balanced with the time-averaged resistive force generated by a cross-bridge that is attached to actin, but not generating active force. Let's call the active force in this situation "sliding force." We estimated the relative magnitude of sliding force as follows. We measure the average sliding velocity, V_s, as a function of ρ. V_s would decrease with increasing ρ. The intercept of the initial tangent of the V_s versus ρ relationship to the abscissa gives a value of $\rho = \rho_s$. The ρ_s value is taken as the relative magnitude of sliding force. The theoretical basis of this method is given in the Discussion.

RESULTS

Sliding Velocity as a Function of NTP Concentration

Sliding velocity, V_s, of actin filaments was measured in an in vitro motility assay using various NTPs. Various nucleotides have different affinities for HMM and acto-HMM (Pate et al., 1993; White et al., 1993). Rigor complexes of acto-HMM, even when in small fractions, may produce resistive drag force against actin filaments sliding, resulting in a reduction of the velocity. To estimate the full ability of each NTP to support acto-HMM motility without rigor complexes and to estimate the apparent Michaelis-Menten constant for each NTP (K_s^N: NTP concentration at which V_s is half of its maximum value), V_s was measured at various NTP concentrations. Fig. 1, a and b give plots of V_s versus [NTP]. At first glance, V_s seemed to show Michaelian saturation as a function of [NTP], i.e., $V_s = V_s^{max}/(1 + K_s^N/[NTP])$. Similar experiments have previously been made with ATP (Sheetz et al., 1984; Homsher et al., 1992; Umemoto and Sellers, 1990; Warshaw et al., 1990; Harada et al., 1987) and with the other nucleotides (Cooke and Bialek, 1979; Pate et al., 1993; Regnier et al., 1998). Some of these studies, where data of V_s versus [MgNTP] have been analyzed quantitatively, have assumed Michaelian saturation behavior. Careful inspection of these and our own data showed that they did not exactly obey the Michaelian relationship. At [NTP] lower than K_s^N, V_s tends to deviate downward from the Michaelian fitting curve. However, at [NTP] moderately higher than K_s^N, V_s tends to deviate upward (see, e.g., Fig. 5 in Homsher et al., 1992; Fig. 3 in Tawada and Sekimoto, 1991). A theoretical consideration regarding this issue under a certain condition led to a mixture of a modified Michaelian equation, i.e., $V_s = V_s^{max}/(1 + (K_s^N)^2/[NTP]^2)$ and the original Michaelian equation (see Discussion). So, we assumed a modified saturation behavior, $V_s = V_s^{max}/(1 + (K_s^N)^n/[NTP]^n)$, where the parameter, n, is one of the parameters to be determined from a least-squares fitting of the data to this modified Michaelian
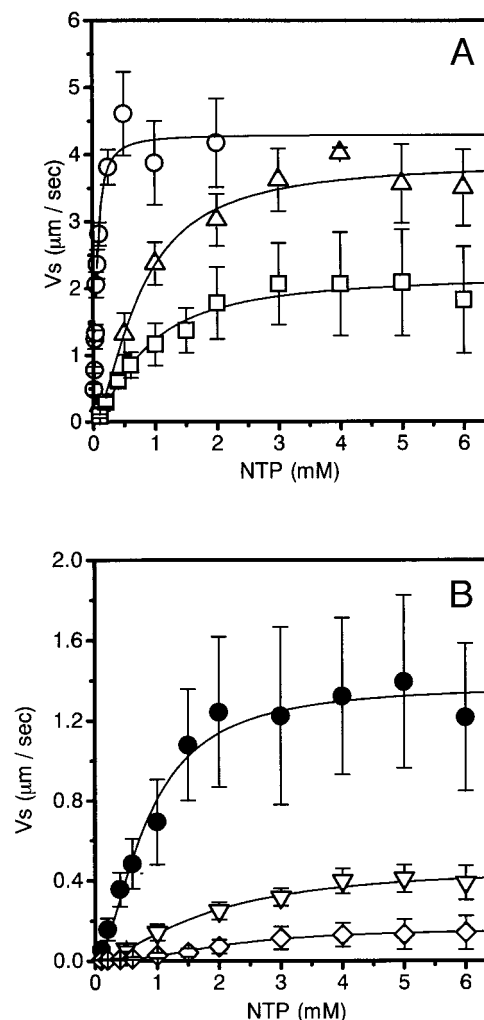

FIGURE 1 Substrate concentration dependence of velocity of actin filament translocation over HMM for (a) ATP ($\bigcirc$), CTP ($\triangle$), TTP ($\square$); and (b) UTP ($\bullet$), GTP ($\triangledown$), and ITP ($\diamond$). Lines are fits to the modified Michaelian equation with n as a variable to be determined, i.e., $V_s = V_s^{max}/(1 + (K_s^N)^n/[NTP]^n)$.

equation. As listed in Table 2, the value of n varied from 1.4 to 2.2 depending on the data, the average value being 1.66. The results are summarized in Table 2, together with the results obtained from the Michaelian data fitting. The standard deviations and χ^2 tests were always smaller when the modified Michaelian saturation with n as a variable was assumed than when the original Michaelian saturation was assumed (Table 2). Although we hereafter describe only values for V_s^{max} and K_s^N obtained with the modified Michaelian data fitting, there were no major differences in the corresponding values obtained with the two types of data fitting (except for the case with ITP).

The value of V_s^{max} for CTP was similar to that obtained with ATP. This similarity was observed previously in in vitro motility assays (Regnier et al., 1998), although in muscle fibers CTP produces shortening velocity 30–50%

TABLE 2   Kinetic parameters of NTP hydrolysis in solution and mechanical properties in the actin sliding assays obtained using various NTPs as substrate

	ATP	CTP	TTP	UTP	GTP	ITP
n*	1.42	1.58	1.41	1.74	1.57	2.23
χ^2 tests*	0.064	0.058	0.018	0.0067	0.00045	0.00003
V_s^{max} (μm/s)*	4.3 ± 0.18	3.9 ± 0.27	2.2 ± 0.16	1.38 ± 0.07	0.47 ± 0.05	0.16 ± 0.01
K_s^N (mM)*	0.059 ± 0.006	0.76 ± 0.12	0.83 ± 0.14	0.82 ± 0.09	1.76 ± 0.35	2.10 ± 0.18
V_s^{max} (μm/s)[†]	4.6 ± 0.21	4.5 ± 0.32	2.5 ± 0.17	1.68 ± 0.14	0.66 ± 0.09	0.37 ± 0.12
K_s^N (mM)[†]	0.07 ± 0.02	0.97 ± 0.25	1.12 ± 0.23	1.19 ± 0.29	3.34 ± 1.0	8.7 ± 4.0
χ^2 tests[†]	0.096	0.079	0.023	0.014	0.00074	0.00012
V_{max} (s^{-1})[‡]	23.6	22.0	18.5	13.5	1.8	4.71
K_m^A (μM)	29.1	28.6	12.0	6.87	0.27	8.0
K_m^N (mM)	0.009	0.11	0.25	0.20	0.50	1.00
V_{HMM} (s^{-1})[§]	0.05	0.038	0.075	0.18	0.35	0.50
ρ_s	0.144	0.118	0.159	0.207	0.169	0.177
$\langle f_s \rangle$ (pN)	0.648	0.531	0.716	0.932	0.76	0.800
k_{+w}/λ_w (M^{-1} s^{-1})	6.8×10^7	7.7×10^7	7.7×10^7	6.5×10^7	6.9×10^8	7.5×10^6
k_{-w}/λ_w (s^{-1})	1992	2202	922	444	185	60

*Obtained by fitting data in Fig. 1, *a* and *b* to the modified Michaelian equation with *n* as a variable.

[†]Obtained by fitting data in Fig. 1, *a* and *b* to the original Michaelian equation (i.e., *n* = 1).

[‡][§]The unit is Pi/s per head.

less than those obtained with ATP (Pate et al., 1993; Wahr and Metzger, 1998). The K_s^N for ATP agreed with published values (Cooke and Bialek, 1979; Ferenczi et al., 1984; Homsher et al., 1992; Regnier et al., 1998). The values of K_s^N for CTP, TTP, and UTP were quite similar to each other (~0.8 mM, 14 times greater than for ATP), while the values of V_s^{max} for these NTPs varied over a relatively wide range. This indicates that the apparent affinity of NTP for acto-HMM does not correlate with V_s^{max}. The values of K_s^N for GTP and ITP were >29 times larger than for ATP, and these nucleotides were poor substrates for producing the sliding motion of actin filaments, as was previously observed with muscle fibers (Pate et al., 1993; Regnier et al., 1998) and in the in vitro motility assays (Regnier et al., 1998; Higashi-Fujime and Hozumi, 1996).

Kinetic parameters of acto-HMM NTPase

At a given concentration of NTP the acto-HMM NTPase activity, V_{NTP}, was measured at various actin concentrations. The NTPs used here were the same as used above. With all the NTPs used V_{NTP} displayed simple hyperbolic saturation behavior as a function of [actin] (data not shown). When the relationship of V_{NTP} versus [actin] was analyzed with the modified Michaelian equation, with *n* as a variable to be determined, we obtained *n* = 1.0 on the average. The values of V_m^A (V_{NTP} at infinite actin concentration) and $K_{0.5}^A$ ([actin] at which V_{NTP} is half of V_m^A) for all six nucleotides were obtained by analyzing the hyperbolic saturation curves by the least-squares criterion to fit the equation $V_{NTP} = V_m^A/(1 + K_{0.5}^A/$ [actin]). Although these parameters, V_m^A and $K_{0.5}^A$, must be less sensitive to the presence of a small amount of rigor complexes than V_s, they (except for those with ATP) may not be saturated in the presence of a millimolar concentration of NTP. We,

therefore examined these parameters as a function of NTP concentration. V_m^A and $K_{0.5}^A$ with CTP were nearly saturated at 1 mM CTP. However, these parameters with TTP, UTP, GTP, and ITP were not saturated at 1 mM [substrates]. V_m^A displayed Michaelian saturation behavior as a function of [MgNTP]. $K_{0.5}$ versus [MgNTP] also showed Michaelian saturation behavior. From these saturation curves V_{max} (V_{NTP} at infinite [NTP] and infinite [actin]) and K_m^A ($K_{0.5}^A$ at infinite [NTP]) were estimated. These values are listed in Table 2. Both V_{max} and K_m^A decreased in the same order, ATP > CTP > TTP > UTP > ITP > GTP, with K_m^A varying more widely than V_{max}. The NTP concentrations, K_m^N, at which V_m^A is half of V_{max}, are also listed in Table 2. K_m^N with ATP was 9 μM, 6.6 times less than the value of K_s^N. K_m^N with CTP could not be accurately determined because this value seemed so small and the hydrolysis rate is so high that V_m^A could not be measured at low concentrations of [MgCTP] (effective CTP-regeneration systems are not available). This parameter, however, seemed to be ~0.1 mM, 6.9 times less than the value of K_s^N. TTP, UTP, and GTP gave values of K_m^N that were in the submillimolar range, 3–4 times less than the respective values of K_s^N. The value of K_m^N for ITP was 1 mM, 2.1 times less than the value of K_s^N. Thus the ratio, K_s^N/K_m^N, is markedly dependent on NTP. The values obtained for the NTPase activity of HMM alone, V_{HMM}, at 6 mM [NTP] are also listed in Table 2. V_{HMM} increased in the order CTP < ATP < TTP < UTP < GTP < ITP, approximately the inverse order to those with V_{max} and K_m^A.

Comparison of motile activity and NTPase kinetics with various NTPs

Here, we examine the relationships between the sliding velocity and the kinetic parameters obtained above. Two kinds of plots, (*a*) V_s^{max} versus V_{max} and (*b*) V_s^{max} versus K_m^A,

are given with open circles and with circles with a cross in Figs. 2 and 3, respectively. Although the curve of V_s^{max} versus V_{max} relationship was concave downward, it suggests a strong correlation between the rate of hydrolysis and the sliding velocity. Previous studies with muscle fibers have reported only moderate correlations between the maximum rate of actin-activated hydrolysis of NTPs by acto-S1 or acto-HMM and the unloaded shortening velocity of muscle fibers (White et al., 1993; Pate et al., 1993; Regnier et al., 1998). In these studies, however, the solution conditions were different in the mechanical and enzymatic measurements, and the concentrations of NTP used for measurements of the hydrolysis rates were fixed at 1 mM, irrespective of the NTP used. Moderate or very poor correlations were also reported in studies with the in vitro actin filament sliding assays (Higashi-Fujime and Hozumi, 1996; Regnier et al., 1998). In the study reporting very poor correlation (Higashi-Fujime and Hozumi, 1996), the hydrolysis rate was measured at a fixed concentration of actin (3.6 μM). A correlation as good as is observed here between the sliding velocity and apparent K_m for actin (K_m^A) (Fig. 3) has never been reported before. Similar examinations have been done previously using various NTPs in muscle fibers and in in vitro motility assays (White et al., 1993; Pate et al., 1993; Regnier et al., 1998). However, results similar to ours were not observed. This may be in part because the previous studies used different solution conditions for measuring the sliding velocity and the enzymatic kinetics.

We have to be careful in concluding that the two excellent correlations shown with open circles and circles with a cross in Figs. 2 and 3 are significant. The two kinetic
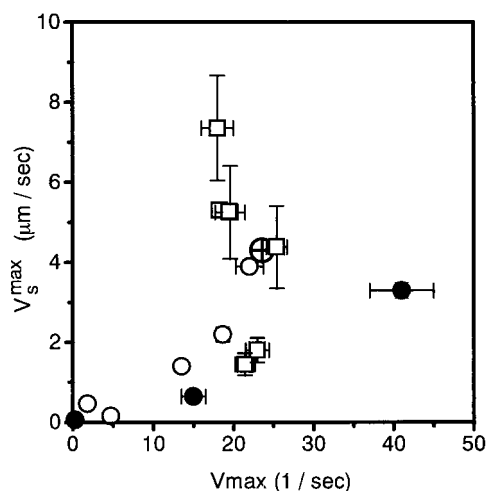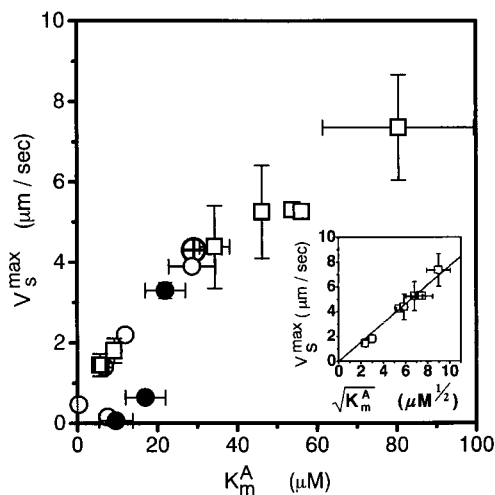

FIGURE 3 The relationship between the maximum sliding velocity (V_s^{max}) and the K_m for actin (i.e., K_m^A). The substrate was altered with MgATP ($\oplus$), MgCTP, MgTTP, MgUTP, MgGTP, MgITP ($\bigcirc$), or with MnATP, NiATP, SrATP ($\bullet$). The ionic strength was altered with KCl ($\square$, $\oplus$). In this case MgATP was used as substrate. The values of K_m^A are those at infinite [NTP]. The inset is the relationship between V_s^{max} vs. $\sqrt{K_m^A}$ obtained when ionic strength was varied.

parameters, V_{max} and K_m^A are, in principle, independent of each other. Yet, they varied in a similar way when the substrate was altered with various MgNTPs. It is, therefore, possible that only one of the two types of correlations is significant, and that another is just accidental. To clarify this aspect we have to perturb the acto-HMM system by other methods and examine the two relationships again.

Motility and kinetics with substrates, ATP complexed with various divalent cations

As second perturbants of the acto-HMM system we used substrates, ATP complexed with various divalent cations (Me^{2+}). We chose Mg^{2+}, Mn^{2+}, Ni^{2+}, and Sr^{2+} for the Me^{2+}. All of these ions, with ATP, supported movement of actin filaments over HMM. First, we measured the dependence of sliding velocity on the substrate concentration. The data for the four substrates were analyzed by least-squares fitting to the modified Michaelian equation with n as a variable to be determined (i.e., $V_s = V_s^{max}/(1 + (K_s^N)^n/[S]^n)$) and to the original Michaelian equation. The results are summarized in Table 3. The standard deviations and χ^2 tests were again often smaller with the former analysis than the latter. Because of this we choose the results obtained from the modified Michaelian data fitting. The data for V_s^{max} yielded the relationship Mg > Mn > Ni > Sr. MnATP was an effective substrate, its V_s^{max} being 77% of that with MgATP. SrATP was a very poor substrate, its V_s^{max} being <2% of that with MgATP. These substrates showed relatively high affinities for acto-HMM, and their values of K_s^N

FIGURE 2 The relationship between the maximum sliding velocity (V_s^{max}) and the maximum acto-HMM NTPase activity (V_{max}, Pi/s/head). The substrate was altered with MgATP ($\oplus$), MgCTP, MgTTP, MgUTP, MgGTP, MgITP ($\bigcirc$), or with MnATP, NiATP, SrATP ($\bullet$). The ionic strength was altered with KCl ($\square$, $\oplus$). In this case MgATP was used as substrate. The maximum acto-HMM NTPase activities are those at infinite [NTP] and infinite [actin].

TABLE 3 Kinetic parameters of Me^{2+} ATP hydrolysis in solution and mechanical properties in the actin sliding assays obtained using various divalent cations as agents complexing with ATP

	MgATP	MnATP	NiATP	SrATP
n^*	1.42	1.25	2.32	1.52
χ^2 tests*	0.064	0.029	0.0082	0.00004
V_s^{max} (μm/s)*	4.3 ± 0.18	3.3 ± 0.17	0.65 ± 0.03	0.065 ± 0.007
K_s^N (mM)*	0.059 ± 0.006	0.18 ± 0.03	0.47 ± 0.09	0.67 ± 0.17
V_s^{max} (μm/s)†	4.6 ± 0.21	3.5 ± 0.15	0.73 ± 0.1	0.073 ± 0.007
K_s^N (mM)†	0.07 ± 0.02	0.20 ± 0.04	0.36 ± 0.23	0.83 ± 0.28
χ^2 tests†	0.096	0.031	0.015	0.00004
V_{max} (s^{-1})‡	23.6	41.0	15.0	0.29
K_m^A (μM)	29.1	22.0	17.0	9.6
V_{HMM} (s^{-1})§	0.05	0.67	0.5	0.023
ρ_s	0.144	0.12	0.14	N.D.
$\langle f_s \rangle$ (pN)	0.648	0.54	0.63	N.D.
k_{+w}/λ_w ($M^{-1}\ s^{-1}$)	6.8×10^7	8.3×10^7	1.82×10^7	N.D.
k_{-w}/λ_w (s^{-1})	1192	1826	309	N.D.

*Obtained by fitting data (V_s vs. [substrate], not shown except for MgATP) to the modified Michaelian equation with n as a variable.
†Obtained by fitting data (V_s vs. [substrate], not shown except for MgATP) to the original Michaelian equation (i.e., $n = 1$).
‡§The unit is Pi/s per head.

were in the submillimolar range. Because K_m^N must be a few times less than K_s^N, several measurements with these substrates were thereafter made at a fixed substrate concentration, 2 mM, which is sufficient to provide almost complete saturation of the nucleotide binding sites. The acto-HMM Me^{2+} ATPase activity exhibited again a simple hyperbolic saturation behavior as a function of actin concentration. The values V_{max} and K_m^A are listed in Table 3. MnATP gave the highest V_{max}, 1.7 times greater than that for MgATP, while its K_m^A value was smaller than that for MgATP. NiATP was an effective substrate with V_{max}, which was 64% of that obtained with MgATP, and its K_m^A value was about half of that for MgATP. SrATP was a very poor substrate. However, HMM complexed with SrATP or its product had the highest affinity for actin. Plots V_s^{max} versus V_{max}, shown with closed circles and a circle with a cross in Fig. 2, indicate only a moderate correlation between the sliding velocity and the maximum hydrolysis rate of Me^{2+} ATP by acto-HMM. As mentioned above, the MnATPase activity was 1.7 times greater than the MgATPase activity. Nevertheless, the sliding velocity with MnATP was 77% of that with MgATP. The relationship V_s^{max} versus K_m^A, shown with closed circles and a circle with a cross in Fig. 3, however, indicated that the sliding velocity was highly correlated with K_m^A, although the fitted line did not intercept the origin. The hydrolysis rates, V_{HMM}, of these Me^{2+} ATP by HMM alone are also listed in Table 3. The $1/V_{HMM}$ increased in the order SrATP < MgATP < NiATP < MnATP. This order was quite different from that of V_s^{max}, indicating no correlation between the two quantities.

Comparison of motile activity and MgATPase kinetics at various ionic strengths

As a third perturbant of the acto-HMM system, we chose differing ionic strengths. When ionic strength in the in vitro

motility assays is higher than ~80 mM, actin filaments or myosin-coated beads tend to dissociate from the respective partners. At lower ionic strengths the rate of movement increases with increasing ionic strength (Harada et al., 1987; Umemoto and Sellers, 1990; Warshaw et al., 1990; Takiguchi et al., 1990; Vale and Oosawa, 1990; Homsher et al., 1992; Saito et al., 1994). With the help of methylcellulose, which reduces the lateral diffusion of actin filaments from the myosin-coated surface (Uyeda et al., 1990), the sliding velocity of actin filaments can increase as ionic strength is elevated even higher than 80 mM (Homsher et al., 1992). Despite general acceptance of this acceleration effect of ionic strength, quantitative analysis of the effect has not been performed, and therefore the underlying mechanism has not been well understood. Here, we reexamined the ionic strength effect on the rate of actin filament translocation. The ionic strength of solution was varied with KCl. MgATP was used as substrate and its concentration was fixed at 2 mM. As shown in Table 4, V_s^{max} increased smoothly with increasing [KCl], with a slight upward deviation from a linear relationship. The maximum rate (V_{max}) of MgATP hydrolysis by acto-HMM was nearly constant over [KCl] from 5 mM to 50 mM (Table 4). K_m^A was, however, increased with increasing [KCl], with upward deviation at higher [KCl] from a linear relationship (Table 4). These distinct behaviors of V_{max} and K_m^A as a function of [KCl] made the relationships V_s^{max} versus V_{max} and V_s^{max} versus K_m^A very different (*squares* and *circles with a cross* in Figs. 2 and 3, respectively). V_s^{max} varied widely, without almost no changes in V_{max}. In contrast to this, V_s^{max} increased with increasing K_m^A. The MgATPase activity of HMM alone, V_{HMM}, increased, in a linear manner, with increasing [KCl] (Table 4). This enhancement effect of [KCl] gave a relationship between V_s^{max} versus V_{HMM} that was completely opposite to that observed when the substrate was altered with various MgNTPs (Table 2).

TABLE 4 Kinetic parameters of MgATP hydrolysis in solution and mechanical properties in the actin sliding assays obtained under various ionic strengths

[KCl] (mM)	V_s^{max} (μm/s)	V_{max}* (s^{-1})	K_m^A (μM)	V_{HMM}[†] (s^{-1})	ρ_s	$\langle f_s \rangle$ (pN)	$\epsilon V_{max}/V_s^{max}$[‡] (pN)	$\sqrt{V_{max}/K_m^A}$ $(s \cdot \mu M)^{-1/2}$
5	1.45	21.4	5.7	0.043	0.20	0.9	1.36	1.94
10	1.81	23.0	9.1	0.042	0.17	0.77	1.16	1.59
25	4.00	23.6	29.1	0.060	0.144	0.65	0.54	0.90
30	4.38	23.1	37.0	0.065	0.115	0.52	0.49	0.79
40	5.25	19.6	46.2	0.065	0.108	0.49	0.34	0.65
43	5.30	18.3	53.9	0.065	0.123	0.55	0.31	0.58
46	5.26	19.5	56.2	0.070	0.126	0.56	0.34	0.59
50	7.35	18.9	70.6	0.065	0.117	0.52	0.24	0.52

*[†]The unit is Pi/s per head.

[‡]ϵ is the work done by one shot of power stroke. The value used is 9.2×10^{-20} J (see Discussion).

Sliding force

It has been recognized that actin filaments would not slide smoothly over HMM when the HMM sample is partially damaged. Based on this phenomenon, Haeberle developed a method for estimating relative magnitude of active force exerted on actin filaments in the in vitro motility assays (Haeberle, 1994). Chemically damaged and therefore noncycling HMM that is mixed with intact HMM imposes an external load on sliding actin filaments and thereby slows the sliding motion. When the molar ratio (ρ) of noncycling HMM to intact HMM is increased with keeping the total HMM amount constant, the movement of actin filaments is eventually stalled. We prepared noncycling HMM by extensively treating HMM with NEM. This NEM-HMM had neither Ca^{2+} NTPase nor actin-activated NTPase activities. Actin filaments attached to the surface that had been coated with this damaged HMM never detached from the surface in the presence of any Mg^{2+}-NTPs. NEM-HMM, therefore, seemed unable to associate with NTP.

We estimated the relative magnitude of active force that is generated by a cross-bridge when cross-bridges are propelling actin filaments to slide without external load or under a small external load. We call this active force "sliding force." The method for this estimation and the basis of this method are described in Materials and Methods and Discussion, respectively. In the first set of experiments we studied the dependence of the relative magnitude of sliding force on NTPs. The concentration of NTP was first fixed at 2 mM. The sliding velocity decreased linearly with increasing ρ, as demonstrated in the inset of Fig. 4. The intercept to the abscissa (i.e., ρ_s) of the initial tangent of the V_s versus ρ, which is supposed to be proportional to the magnitude of sliding force, was roughly constant over the NTPs used (Fig. 4 and Table 2). Since 2 mM of NTPs (except for ATP) do not saturate the nucleotide binding site of HMM, these measurements were repeated at various concentrations of NTP (from 1 to 6 mM). We could not, however, find NTP-concentration dependence of the ρ_s values, even with GTP and ITP, whose affinities for acto-HMM were low compared with the other NTPs. Also in the

second set of experiments, where divalent cations that complex with ATP were varied, the ρ_s values were quite similar to each other (Table 3). In this experiment Sr^{2+} ATP was omitted because of the very small rate of movement. In the third set of experiments, where MgATP was used as substrate and the ionic strength was varied with various [KCl], ρ_s showed a tendency to decline with increasing [KCl] (Table 4). In this experiment the resistive force by NEM-HMM may vary depending on [KCl]. It is likely that the higher [KCl] may result in less resistive force. The tendency for sliding force to decline with increasing [KCl] may, therefore, be more significant than that of ρ_s.

DISCUSSION

A kinetic scheme of the actomyosin ATPase

Before we discuss the experimental results obtained in the present study, we briefly describe the kinetics of the acto-
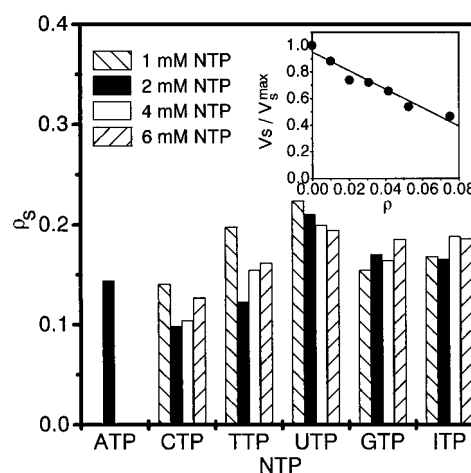
FIGURE 4 Relative magnitude of sliding forces in various MgNTPs and its dependency on [MgNTP]. The ionic strength was kept constant by adjusting [KCl]. The inset shows dependence of sliding velocity in MgATP upon the molar ratio (ρ) of NEM-HMM to intact HMM. The linear line intercepts the abscissa at $\rho = \rho_s$.

myosin ATPase reaction. The kinetic scheme shown here accounts for the results of various kinetic experiments. Myosin heads are distinguished according to their actin-binding kinetics (Stein et al., 1979), i.e., "weak-binding states" and "strong-binding states." ATP binds to a rigor cross-bridge (step 1) to form a weakly bound state (A · M · ATP), followed rapidly by dissociation of actin (A) from myosin (M) (step 2), or by hydrolysis of the γ-phosphate (step 3). After hydrolysis of the γ-phosphate (step 3 and step 5), a weakly bound state (A · M · ADP · Pi) forms, which is in a rapid equilibrium with the M · ADP · Pi state (step 4). The weakly bound cross-bridge then isomerizes to a strong-binding state (step 6). The bound phosphate is released (step 7) to form A · M* · ADP, which is followed by isomerization (step 8). Finally, ADP is released (step 9) to form a rigor cross-bridge. Rate limitation of the ATPase cycle in solution has been variously thought to occur at the isomerization step (step 6) (Stein et al., 1979, 1984), at the Pi release step (step 7) (Webb and Trentham, 1981; Hibberd and Trentham, 1986; Barman et al., 1998) (the two states, A · M · ADP · Pi and A · M* · ADP · Pi, are not distinguished), or at the cleavage step (step 3) (Rosenfeld and Taylor, 1984; White et al., 1997) (deduced from observations that a high concentration of actin suppresses the ATPase activity at very low ionic strength). Using a fluorescent Pi-probe and caged-ATP in single muscle fibers, He et al. (1997, 1998) have observed that the onset of tension development is slightly earlier than that of Pi release, indicating that A · M* · ADP · Pi contributes to the force-generating state. Other studies have also presented evidence that both A · M* · ADP · Pi and A · M* · ADP contribute to the force-generating state (Lund et al., 1987; Dantzig et al., 1992; Cooke, 1995). Although a consensus about the rate-limiting step in the ATPase cycle has not been reached, it has been generally accepted that 1) myosin heads reside predominantly in the weak-binding state(s) in which they are in a rapid equilibrium between the actin-attached and detached states, and 2) an intermediate just after the power stroke is A · M · ADP. Although in a part of the subsequent discussion we assume the rate-limiting step to be step 6, we do not intend to validate this assumption. The results given below are not strongly associated with this assumption. The ATPase kinetic scheme cited here probably hold for almost all the other nucleotides, as suggested by Pate et al. (1993);
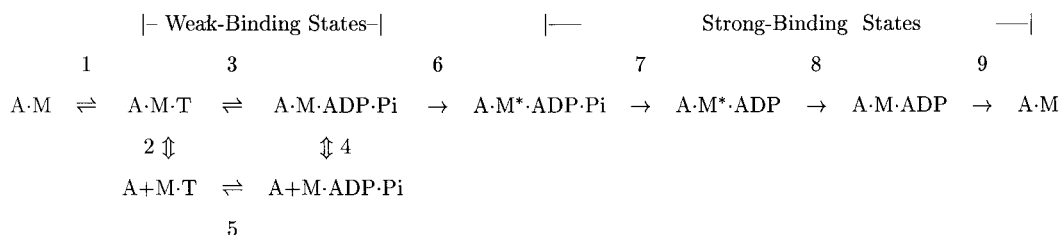
White et al. (1993); and Regnier et al. (1998); although the GTPase probably has a different kinetic mechanism (Eccleston and Trentham, 1979; White et al., 1997).

Resistive drag forces

Actin-attached cross-bridges that are not executing the power stroke produce a resistive force opposing sliding movement, because these cross-bridges are pulled and deformed passively by moving actin filaments. In a high concentration of substrate, such resistive cross-bridges are in the post-power stroke state (from which NDP is released) and in the weak-binding states. To the authors, it seems controversial whether weakly bound cross-bridges produce resistive force to such an extent that it affects or determines the sliding velocity (Warshaw et al., 1990; Homsher et al., 1992; Cuda et al., 1997; Brenner, 1990). First, we examine this issue quantitatively, since this issue seems to have the key to understanding the link between the chemistry and the mechanics in skeletal actomyosin. If for a time T a resistive cross-bridge remains attached to a sliding actin filament (velocity, V_s), it is pulled for a distance of V_sT. When averaged over the cycle time ($T_c = 1/V_{max}$) of the NTPase reaction, the resistive force, f_r, becomes

$$\langle f_r \rangle = \frac{1}{2}\lambda\Gamma V_sT \qquad (1)$$

where Γ is an elastic constant of a resistive cross-bridge and λ is the fraction of this resistive state over all states. Now, we roughly estimate the magnitude of $\langle f_r \rangle$ in ATP, using values of λ, Γ, and T. Although Γ may vary depending on the state concerned, the reported values for different states are similar to each other: 0.65 pN/nm, measured directly using a single-molecule technique in the midst of an ATPase cycle (Mehta et al., 1997); 0.58 pN/nm, measured directly using a single-molecule technique in the rigor state (Nishizaka et al., 1995). So, we assume $\Gamma = 0.6$ pN/nm for all the resistive states. For weakly bound cross-bridges, the time, T, equals $1/k_{-2}$ or $1/k_{-4}$. Hereafter, we assume $k_{-2} = k_{-4}$ ($\equiv k_{-w}$) and $k_{+2} = k_{+4}$ ($\equiv k_{+w}$). The rate constant of dissociation of myosin heads with ATP from actin is likely to be ~2000 s^{-1}, inferring from the values obtained previously under various solution conditions. So, we assume $T = 0.5$ ms. Skeletal actomyosin has a low duty ratio, the frac-

|– Weak-Binding States–| |——   Strong-Binding States   ——|

1   3   6   7   8   9

A·M   ⇌   A·M·T   ⇌   A·M·ADP·Pi   →   A·M*·ADP·Pi   →   A·M*·ADP   →   A·M·ADP   →   A·M

   2 ⇕   ⇕ 4

   A+M·T   ⇌   A+M·ADP·Pi

   5

Scheme 1

tion of time that a cross-bridge spends generating active force. The ratio is suggested to be ~0.1 (Cooke, 1997), and myosin heads reside predominantly in the weak-binding state(s). Taking these features into account, the total fraction of weakly bound cross-bridges is supposed to be ~0.8. These values for Γ, T, λ, and $V_s = 4.3$ μm/s result in $\langle f_r \rangle = 0.51$ pN per a weakly bound cross-bridge. As will be shown later, this magnitude is comparable to the time-averaged active force per a cross-bridge, but significantly lower than the force required to unbind a rigor head from actin. The lifetime of the post-power stroke state is determined by the rate constant of ADP dissociation from the actin-bound cross-bridge (here we distinguish the resistive forces produced by A · M · ADP and A · M · ATP. The latter is counted among those produced by weakly bound cross-bridges.) Although the rate constant of ADP dissociation on the ATP hydrolysis pathway has not been determined, we assume that it is similar to the rate constant (k_{-AD}) of ADP dissociation from the state formed by externally adding ADP to actomyosin. For rabbit skeletal actomyosin, k_{-AD} is ~1000 s^{-1} (700–1000 s^{-1} at 25°C, Siemankowski et al., 1985; 1400 s^{-1} at 20°C, Borejdo et al., 1985). So, we assume $T = 1$ ms. The fraction of the post-power stroke state is supposed to be very small (Barman et al., 1998). Tentatively, we assume $\lambda = 0.023$, because λ must equal $T/T_c = 1/42$ ($T_c = 1/V_{max} = 42.4$ ms). These values lead to a rough estimate, $\langle f_r \rangle = 0.029$ pN, 17.6 times less than that produced by a weakly bound cross-bridge. We have to note here that a cross-bridge in the post-power stroke state produces a resistive force just once during an ATPase cycle, while in the weak-binding states a cross-bridge produces it many times. Here, for simplicity, we neglected the reductive effect of elastic deformation on the lifetime (T) of weakly bound cross-bridges. The rate of ADP dissociation may be affected by the elastic deformation. Here, we do not consider it. When the deformation energy, $E_d = 0.5 \times \Gamma(V_s T)^2$, is comparable to or larger than the thermal energy, $E_0 \sim 4 \times 10^{-21}$ J, T should be reduced significantly, as has been demonstrated in the acto-HMM rigor bond (Nishizaka et al., 1995). The deformation accelerates the rate of dissociation from actin by a factor of e^{E_d/E_0} (Bell, 1978). So, the probability of finding a cross-bridge that bound to actin at time zero and keeps associating with actin till time t is proportional to $P(t) \equiv \exp(-\int_0^t k_{-w} e^{E_d/E_0} dt)$. Therefore, the lifetime, T, can be determined by $T = \int_0^\infty t\, P(t) dt / \int_0^\infty P(t) dt$. Performing the integrations numerically, we find that the lifetime of a weakly bound cross-bridge is slightly reduced to 0.3 ms (the resistive force, 0.31 pN). A slight increase in the dissociation rate hardly affects the fraction of weakly bound cross-bridges because a high concentration of actin shifts the rapid equilibrium to the actin-attached side. Although the difference in the resistive forces produced in the weak-binding states and in the post-power stroke state became smaller (10.7 times), it is still large. Even when we choose a lower value, 700 s^{-1}, for the ADP dissociation rate

(λ becomes 0.034), the difference in the resistive forces is still 5 times. After all, we reached an estimate that resistive force is produced predominantly by weakly bound cross-bridges. Hereafter, we neglect resistive forces produced by cross-bridges in the post-power stroke state. We also neglect the deformation effect on the lifetime of weakly bound cross-bridges, because it is not so large. As will be seen later, deformation energy stored in weakly bound cross-bridges is rather independent of nucleotides (a longer life-time and a slower rate of movement cancel out each other to give a similar deformation energy).

Dependence of sliding velocity on substrate concentration

Sliding velocity (V_s) of actin filaments decreases with decreasing substrate concentration, [S] (Fig. 1, *a* and *b*). This is certainly due to the resistive forces produced by the nucleotide-free rigor cross-bridges (i.e., AM). The lifetime, T_{rig}, of an AM rigor cross-bridge is determined by

$$T_{rig} = 1/(k_{+1}[S]), \tag{2}$$

where k_{+1} is the second-order rate constant of nucleotide binding. When averaged over $T_{rig} + T_c$, the resistive force per an AM rigor cross-bridge is given by

$$\lambda_{rig} \times \tfrac{1}{2}\Gamma V_s T_{rig}, \tag{3}$$

where $\lambda_{rig} = T_{rig}/(T_{rig} + T_c)$, and $\Gamma V_s T_{rig}$ cannot exceed the force (F_u) required to rupture an AM rigor cross-bridge. If it exceeds F_u, the average resistive force should be replaced with $0.5 \times \lambda_{rig} F_u$. For a while we consider the case where $\Gamma V_s T_{rig} < F_u$ holds. Including the resistive force produced by a weakly bound cross-bridge, a balance of the time-averaged forces regarding one cross-bridge is expressed as follows.

$$\frac{T_c}{T_{rig} + T_c}\langle f_s \rangle = \frac{T_c}{T_{rig} + T_c} \times \frac{1}{2}\lambda_w \Gamma V_s T_w$$
$$+ \frac{T_{rig}}{T_{rig} + T_c} \times \frac{1}{2}\Gamma V_s T_{rig}, \tag{4}$$

where $\langle f_s \rangle$ is sliding force (active force) averaged over T_c, λ_w is the fraction of weakly bound cross-bridges in T_c, and $T_w (\equiv 1/k_{-w})$ is the lifetime of weakly bound cross-bridges. This equation is independent of the concentration of HMM on the coverslip (above certain threshold level). Solving this equation for V_s, we obtain

$$V_s = \frac{2\langle f_s \rangle}{\lambda_w \Gamma T_w} \Big/ \left(1 + \frac{T_{rig}^2}{\lambda_w T_w T_c}\right) \tag{5}$$

By substituting $1/k_{-w}$, $1/(k_{+1}[S])$, and $1/V_{max}$ into T_w, T_{rig},

and T_c, respectively, we obtain

$$V_s = \frac{2k_{-w}\langle f_s\rangle}{\lambda_w \Gamma}\Bigg/\left(1 + \frac{k_{-w}V_{max}}{\lambda_w k_{+1}^2 [S]^2}\right)$$

$$= V_s^{max}\Bigg/\left(1 + \frac{(K_s^N)^2}{[S]^2}\right), \qquad (6)$$

where V_s^{max} and K_s^N are respectively defined by

$$V_s^{max} = \frac{2k_{-w}\langle f_s\rangle}{\lambda_w \Gamma} = \frac{2k_{+w}K_m^A\langle f_s\rangle}{\lambda_w \Gamma} \qquad (7)$$

$$K_s^N = \frac{1}{k_{+1}}\sqrt{\frac{k_{-w}V_{max}}{\lambda_w}} = \frac{1}{k_{+1}}\sqrt{\frac{k_{+w}K_m^A V_{max}}{\lambda_w}} \qquad (8)$$

Here, V_s^{max} is the maximum sliding velocity, K_s^N is the substrate concentration at which V_s is half of V_s^{max}, and K_m^A is the actin concentration at which the enzymatic activity is half of V_{max} and approximately equals k_{-w}/k_{+w}. Here, we assumed that $\langle f_s\rangle$ is constant, although it must vary depending on V_s. Equation 6 is the same as the modified Michaelian equation, with $n = 2$. Now, we consider the case where $\Gamma V_s T_{rig} > F_u$ holds. In this case, substitution of F_u for $\Gamma V_s T_{rig}$ in Eq. 4 leads to

$$V_s = V_s^{max}\left(1 - \frac{K_s^N}{2}\Bigg/[S]\right) \quad (V_s > 0), \qquad (9)$$

where V_s^{max} is the same as that in Eq. 7, but K_s^N is newly given by

$$K_s^N = V_{max}F_u/(k_{+1}\langle f_s\rangle) \qquad (10)$$

For a range $[S] \sim K_s^N$, Eq. 9 can roughly be approximated to the original Michaelian equation ($n = 1$) as

$$V_s \simeq V_s^{max}/(1 + K_s^N/[S]) \qquad (11)$$

Equation 6 holds for $[S]$ that satisfies the condition, $F_u > \Gamma V_s T_{rig}$. Putting this condition and $T_{rig} = 1/(k_{+1}[S])$ into Eq. 6, we obtain the following quadratic inequality:

$$[S]^2 - \frac{\Gamma V_s^{max}}{k_{+1}F_u}[S] + (K_s^N)^2 > 0 \qquad (12)$$

Solving this inequality for $[S]$, we find that in the case $F_u > F_0 (\equiv \Gamma V_s^{max}/(2k_{+1}K_s^N))$, any $[S]$ satisfies Eq. 12, while in the case $F_u < F_0$, Eq. 12 can be satisfied by $[S]$ that are higher than $([S]_c + \Delta)$, or lower than $([S]_c - \Delta)$, where $[S]_c$ and Δ are $(F_0/F_u)K_s^N$ and $\sqrt{([S]_c)^2 - (K_s^N)^2}$, respectively. Here, we examine quantitatively whether F_u is smaller or larger than F_0. The magnitude of force required for unbinding a rigor complex of a single head of HMM and actin has been measured by a laser optical trap (Nishizaka et al., 1995), or by atomic force microscopy (Nakajima et al., 1997). In the case where an actin filament is pulled along its length, the unbinding force is about 9 pN (measured in the same ionic

solution as used in the present study with $[KCl] = 25$ mM). The second order rate constant (k_{+1}) of MgATP binding to actomyosin is around 2×10^6 M^{-1} s^{-1} (White and Taylor, 1976; Ando, 1984). So, $F_0 (\equiv \Gamma V_s^{max}/(2k_{+1}K_s^N))$ becomes 11 pN, slightly larger than the unbinding force, $F_u = 9$ pN. This means that at $[MgATP]$ between $([S]_c - \Delta)$ and $([S]_c + \Delta)$, the relationship V_s versus $[MgATP]$ should obey the original Michaelian equation (or Eq. 9), and in the other ranges of $[MgATP]$, it should obey the modified Michaelian equation with $n = 2$. In practice, the borders $([S]_c - \Delta)$ and $([S]_c + \Delta)$ are blurred by stochastic variation of the unbinding force around its average (F_u). The shifts between the two types of Michaelian relationships, therefore, do not occur in discrete steps. This seems to be the reason why the least-squares analysis of our data of V_s versus $[MgATP]$ gave $n = 1.42$ (Table 2). Since analysis of our data of V_s versus $[S]$ (Fig. 1, a and b) gave $n = 1.4$–1.74 for the various nucleotides (except for ITP ($n = 2.23$)), similar balances between F_u and F_0 must hold for these nucleotides.

Now we are going to find the basis for the large difference in the $[NTP]$ dependence of the velocity of actin filaments, and of acto-HMM NTPase activity (Table 2). The NTP concentration, K_s^N, that gives half of the maximum sliding velocity (V_s^{max}), is larger than the NTP concentration, K_m^N, at which the acto-HMM NTPase is half of its maximum (V_{max}). Suppose that isomerization step (step 6) is the rate-limiting step and $k_{+6} \ll k_{+7}, k_{+8}, k_{+9}$, we obtain approximations: $V_{max} \simeq \lambda_w k_{+6}$ and $K_m^N \simeq \lambda_w k_{+6}/k_{+1} = V_{max}/k_{+1}$ (when $k_{-1} \ll k_{+3}$). The condition $k_{-1} \ll k_{+3}$ has been proven to hold for MgATP (Brune et al., 1994). Although these approximations may not hold for the poor substrates, GTP and ITP, let's continue to explicate further. By putting these approximations into Eqs. 8 and 10, K_s^N can be related to K_m^N as

$$K_s^N = K_m^N\sqrt{k_{-w}/k_{+6}}/\lambda_w, \qquad (13)$$

or

$$K_s^N = K_m^N \frac{F_u}{\langle f_s\rangle} \qquad (14)$$

From the relationships, $k_{-w} \gg k_{+6}$ or $F_u \gg \langle f_s\rangle$, we can understand the observed relationship, $K_s^N \gg K_m^N$.

Using $K_m^N \simeq V_{max}/k_{+1}$ and $\lambda_{rig} = T_{rig}/(T_{rig} + T_c) = 1/(1 + k_{+1}[S]/V_{max})$, the modified Michaelian equation gives the relationship of V_s versus λ_{rig}.

$$V_s = V_s^{max}\Bigg/\left(1 + \left(\frac{\lambda_{rig}}{1 - \lambda_{rig}}\right)^n \left(\frac{K_s^N}{K_m^N}\right)^n\right) \quad (1 < n < 2) \qquad (15)$$

The initial slope of V_s/V_s^{max} as a function of λ_{rig} is zero, coinciding with the observation (*open circles* in Fig. 5). The solid line in Fig. 5 was obtained by fitting the data (*closed circles* in Fig. 1 b to Eq. 15. The fitting was not good at higher λ_{rig}, wherein $V_s/V_s^{max} < 0.3$. This arises mainly from
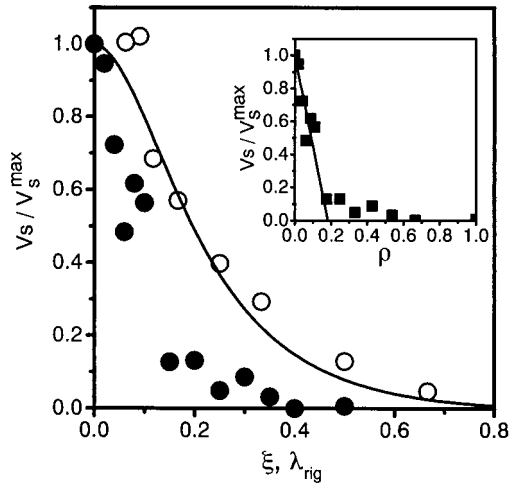
FIGURE 5 Resistive effects of rigor complexes on the velocity of actin filament translocation in assay 1 and assay 2. The substrate was MgUTP. In assay 1, the fraction of rigor complexes (λ_{rig}) was altered by changing the concentration of UTP ($\bigcirc$); while in assay 2, the fraction of rigor complexes (ξ) was altered by mixing various amounts of NEM-HMM with intact HMM while keeping the total amount of NEM-HMM plus intact HMM constant ($\bullet$). In assay 1, the fraction of rigor complexes was calculated using $\lambda_{\text{rig}} = 1/(1 + k_{+1}[S]/V_{\text{max}}) \simeq (K_{\text{m}}^{\text{N}}/[UTP])/(1 + K_{\text{m}}^{\text{N}}/[UTP])$. A line is fit to Eq. 15 with $n = 1.74$. The inset shows the relationship between $V_{\text{s}}/V_{\text{s}}^{\text{max}}$ vs. $\rho(\equiv\xi/(1 - \xi))$ obtained in assay 2.

that $\langle f_{\text{s}}\rangle$ is not constant in this range of λ_{rig}. We observed the resistive effect of nucleotide-free rigor complexes on V_{s} also in a different assay system (assay 2), where noncycling HMM (NEM-HMM) is present together with intact HMM in the presence of [S] that is sufficient to saturate the nucleotide binding sites. As shown in Fig. 5, this resistive effect (*closed circles*) was stronger than that in the previous assay system (assay 1, *open circles*). In assay 2 the force balance equation is given by

$$(1 - \xi)\langle f_{\text{s}}\rangle = (1 - \xi)\tfrac{1}{2}\lambda_{\text{w}}\Gamma V_{\text{s}}T_{\text{w}} + \xi\tfrac{1}{2}F_{\text{u}}, \qquad (16)$$

where ξ is the fraction of NEM-HMM. Solving this equation for V_{s}, we obtain

$$V_{\text{s}} = V_{\text{s}}^{\text{max}}\left(1 - \frac{\xi}{1 - \xi}\frac{F_{\text{u}}}{2\langle f_{\text{s}}\rangle}\right) \qquad (17)$$

The initial slope of $V_{\text{s}}/V_{\text{s}}^{\text{max}}$ as a function of ξ is $-0.5F_{\text{u}}/\langle f_{\text{s}}\rangle$, markedly different from that in assay 1. Equation 17 predicts that plots of V_{s} versus $\rho \equiv \xi/(1 - \xi)$ should give a straight line. As shown in the insets of Figs. 4 and 5, this is true as far as $V_{\text{s}}/V_{\text{s}}^{\text{max}}$ is larger than 0.3. At $V_{\text{s}}/V_{\text{s}}^{\text{max}} < 0.3$, the noncycling HMM is less efficient in reducing the rate of movement, indicating that $\langle f_{\text{s}}\rangle$ increases under a large external load.

Sliding force

From Eq. 17 the sliding force, $\langle f_{\text{s}}\rangle$, equals $0.5\rho_{\text{s}}F_{\text{u}}$, where ρ_{s} is the intercept of the abscissa of the initial tangent in the

relationship of V_{s} versus ρ. The ρ_{s} values with various MgNTPs varied from 0.12 to 0.2 (Fig. 4, Table 2). When divalent cations that complex with ATP were varied, the ρ_{s} values were 0.144, 0.12, and 0.14 for MgATP, MnATP, and NiATP, respectively (Table 3). When [KCl] was varied using MgATP as substrate, ρ_{s} varied from 0.2 to 0.11, with a tendency to decrease with increasing ionic strength (Table 4). The time-averaged magnitude of sliding force with MgATP at 25 mM KCl is estimated to be 0.65 pN ($=0.5 \times 0.144 \times 9$). Force generation by a single myosin head has been measured directly using optical traps (Mehta et al., 1997) or micro-needles (Ishijima et al., 1991, 1996). The magnitude of the power stroke (force spike) has been found to be 2–10 pN, depending on the methods. The higher values seem reliable, considering a compliance problem involved in the single-molecule techniques. So, the maximum power stroke must be 5–10 pN. Since the duty ratio is ~0.1 (Cooke, 1997), the active force per cross-bridge is 0.5–1.0 pN on a time-average, similar to 0.65 pN, the value estimated above as the sliding force. The values of sliding force for the other substrates are listed in Tables 2 and 3. The values vary in a small range around 0.7 pN. A possible mechanism that accounts for the approximate constancy of $\langle f_{\text{s}}\rangle$ over various substrates will be discussed later.

Dissociation and association rate constants

Equation 7 can be re-written as follows.

$$\frac{k_{+\text{w}}}{\lambda_{\text{w}}} = \frac{\Gamma V_{\text{s}}^{\text{max}}}{2K_{\text{m}}^{\text{A}}\langle f_{\text{s}}\rangle} \qquad (18)$$

The right-hand side of this equation contains kinetic and mechanical parameters whose values, except for Γ, were obtained in the present study. As mentioned already, the value of Γ has been estimated to be ~0.6 pN/nm in other laboratories. Using these values (Table 2), we calculated the values of $k_{+\text{w}}/\lambda_{\text{w}}$ and $k_{-\text{w}}/\lambda_{\text{w}}$ using Eq. 18 and $k_{-\text{w}} = k_{+\text{w}}K_{\text{m}}^{\text{A}}$, respectively. The results are listed in Tables 2 and 3. The values of $k_{+\text{w}}/\lambda_{\text{w}}$ for MgATP, MgCTP, MgTTP, and MgUTP were quite similar to each other. Since $k_{+\text{w}}$ and λ_{w} are independent parameters, this similarity suggests that the respective values of $k_{+\text{w}}$ and λ_{w} are similar for these substrates. However, the value $k_{+\text{w}}/\lambda_{\text{w}}$ for MgGTP was one order of magnitude larger than these substrates, while the value for MgITP was one order of magnitude smaller. As mentioned already, this probably arises from different hydrolysis mechanisms of the poor nucleotides. The dissociation rate constant divided by λ_{w} (i.e., $k_{-\text{w}}/\lambda_{\text{w}}$) decreased in the order CTP ≈ ATP > TTP > UTP > GTP > ITP, quite similar to the order with the maximum sliding velocity, $V_{\text{s}}^{\text{max}}$. Because the fraction of weakly bound cross-bridges in ATP is very likely to be 0.8–0.9, the value of $k_{-\text{w}}$ for ATP is 1600–1800 s^{-1} (1992 × 0.8–0.9), similar to those reported previously for the maximum rate of acto-HMM

dissociation (Regnier et al., 1998) or acto-S1 dissociation (White et al., 1993) by ATP, although the previous measurements were made at relatively high ionic strength.

Relationships of V_s^{max} versus V_{max}, and V_s^{max} versus K_m^A

Analysis of changes in V_s^{max} (the maximum sliding velocity) and V_{max} (the maximum substrate turnover rate) depending on MgNTPs (*open circles* and *circle with a cross* in Fig. 2) revealed that these quantities correlated well with each other. When various MeATPs were used as substrates (*closed circles* and *circle with a cross* in Fig. 2), the correlation was poor. When MgATP was used as substrate and ionic strength was varied, V_{max} was nearly constant, while V_s^{max} increased with increasing ionic strength (*squares* and *circle with a cross* in Fig. 2). How can we interpret this result? Before getting into this issue, let's look at the observed relationships between V_s^{max} and K_m^A. The relationship was approximately linear when the substrate was altered with MgNTPs (*open circles* and *circle with a cross* in Fig. 3). When the system with MgATP was perturbed by altering the ionic strength, V_s^{max} increased with increasing K_m^A, with the curve being concave upward (*squares* and *circle with a cross* in Fig. 3). These similar behaviors guarantee that this excellent correlation is not accidental, but intrinsic to the protein motor system. This supports our theoretical result, Eq. 7, that indicates V_s^{max} is proportional to K_m^A (the other parameters contained in Eq. 7, i.e., k_{+w}/λ_w and $\langle f_s \rangle$, are not strongly dependent on nucleotide substrate except for GTP and ITP (Table 2)). A previous study (Regnier et al., 1998) also seems to support this relationship. The rate constant, k_{-2}, estimated from the rate of acto-HMM dissociation after adding NTP, increased in the order CTP < UTP < ATP < dATP, while the shortening speed of fibers increased in the order UTP < ATP ≈ CTP < dATP. Neglecting the data with CTP, the shortening speed linearly increased with increasing k_{-2} (Tables 3 and 4 in Regnier et al., 1998).

The maximum turnover rate, V_{max}, is not visibly contained in Eq. 7. To link V_{max} to the maximum rate of movement (V_s^{max}) we need another perspective. We consider a situation where an actin filament is sliding at maximum velocity on HMM without external load. In this situation, the actin filament receives power stroke(s) from cross-bridges at any moment. Each power stroke (the duration, T_p) displaces the actin filament by a distance, d. However, power strokes by several cross-bridges that happen to overlap at one moment produce the same step displacement, d. According to this model, the power stroke speed (d/T_p) should equal the maximum sliding velocity (V_s^{max}) (Uyeda et al., 1991). The average sliding force per a cross-bridge, $\langle f_s \rangle$, equals pT_p/T_c, where p is the magnitude of power stroke

(force spike). From these relationships we can obtain

$$\langle f_s \rangle = pd \frac{V_{max}}{V_s^{max}} \tag{19}$$

From Eqs. 7 and 19, two mechanical variables, V_s^{max} and $\langle f_s \rangle$, can be expressed separately.

$$V_s^{max} = \sqrt{\frac{2pdk_{+w}}{\lambda_w \Gamma}} \sqrt{K_m^A V_{max}} \tag{20}$$

$$\left(= \sqrt{\frac{2pd}{\Gamma}} \sqrt{k_{-w}k_{+6}} \right)$$

$$\langle f_s \rangle = \sqrt{\frac{pd\lambda_w \Gamma}{2k_{+w}}} \sqrt{\frac{V_{max}}{K_m^A}} \tag{21}$$

$$\left(= \lambda_w \sqrt{\frac{pd\Gamma}{2}} \sqrt{\frac{k_{+6}}{k_{-w}}} \right)$$

These two equations link the mechanical behaviors of actomyosin to the enzymatic properties. They tell us that important parameters of the enzymatic kinetics in the determination of the mechanical behaviors are the dissociation rate constant (k_{-w}) in the weak-binding states and the rate constant of the rate-limiting step (here, we assumed it to be step 6). V_{max} (or k_{+6}) is involved in V_s^{max} and $\langle f_s \rangle$ in the same way, while K_m^A (or k_{-w}) is inversely involved in V_s^{max} and $\langle f_s \rangle$. These two equations successfully account for many of our observations. When the acto-HMM system was perturbed by altering the substrate with various MgNTPs, both K_m^A and V_{max} changed roughly in parallel. So, Eq. 20 predicts approximate linear relationships between V_s^{max} and K_m^A, and between V_s^{max} and V_{max}, under an assumption that $pdk_{+w}/\lambda_w \Gamma$ is approximately constant. This coincides with what we observed (*open circles* and *circles with a cross* in Figs. 2 and 3). When the acto-HMM system in MgATP was perturbed by changing [KCl], V_{max} was nearly constant, while K_m^A increased with increasing [KCl] (Table 4). In this case, Eq. 20 predicts that V_s^{max} increases in proportion to $\sqrt{K_m^A}$. This again approximately coincides with what we observed (the inset of Fig. 3). Equation 21 predicts that $\langle f_s \rangle$ is proportional to $\sqrt{V_{max}/K_m^A}$. As mentioned above, both K_m^A and V_{max} changed roughly in parallel when various MgNTPs were used. Therefore, $\langle f_s \rangle$ should be nearly constant under the assumption that $pdk_{+w}/\lambda_w \Gamma$ is approximately unchanged. This is what we observed (Fig. 4, Table 2). When [KCl] was altered for acto-HMM in MgATP, $\langle f_s \rangle$ declined with increasing [KCl]. As can be seen in Table 4, $\langle f_s \rangle$ was roughly proportional to $\sqrt{V_{max}/K_m^A}$. At [KCl] < 25 mM, however, $\langle f_s \rangle$ was smaller than expected from the corresponding $\sqrt{V_{max}/K_m^A}$ values, while at [KCl] > 25 mM $\langle f_s \rangle$ was larger than expected from the corresponding $\sqrt{V_{max}/K_m^A}$ values. We have to note that the $\langle f_s \rangle$ values have been estimated on the assumption that F_u (measured at 25 mM KCl) is constant irrespective of [KCl]. Corrections of

the $\langle f_s \rangle$ values by a likely dependence of F_u on [KCl] may lead to better agreement.

Equations 20 and 21 predict that plots of V_s^{max} versus $\sqrt{2k_{+w}K_m^A V_{max}/(\lambda_w \Gamma)}$ (the right-hand side of Eq. 20 divided by $\sqrt{pd}$) and plots of $\langle f_s \rangle$ versus $\sqrt{\lambda_w \Gamma V_{max}/(2k_{+w}K_m^A)}$ (the right-hand side of Eq. 21 divided by $\sqrt{pd}$) give straight lines with a slope of $\sqrt{pd}$. As shown in Fig. 6, a and b, this was the case, although the data with the poor substrates were deviated from the straight line (Fig. 6 b). The least-squares analysis of these plots gave $pd = 9.2 \times 10^{-20}$ J (from Fig. 6 a) and $pd = 9.3 \times 10^{-20}$ J (from Fig. 6 b), surprisingly close to the free energy change associated with ATP hydrolysis in living cells, 8.3×10^{-20} J (Stryer, 1981). These linear relationships also indicate that these MgNTPs (except for the poor substrates) are similar to each other in the extent of energy liberation by hydrolysis and in the efficiency of energy transduction (nearly 100%). Here, we
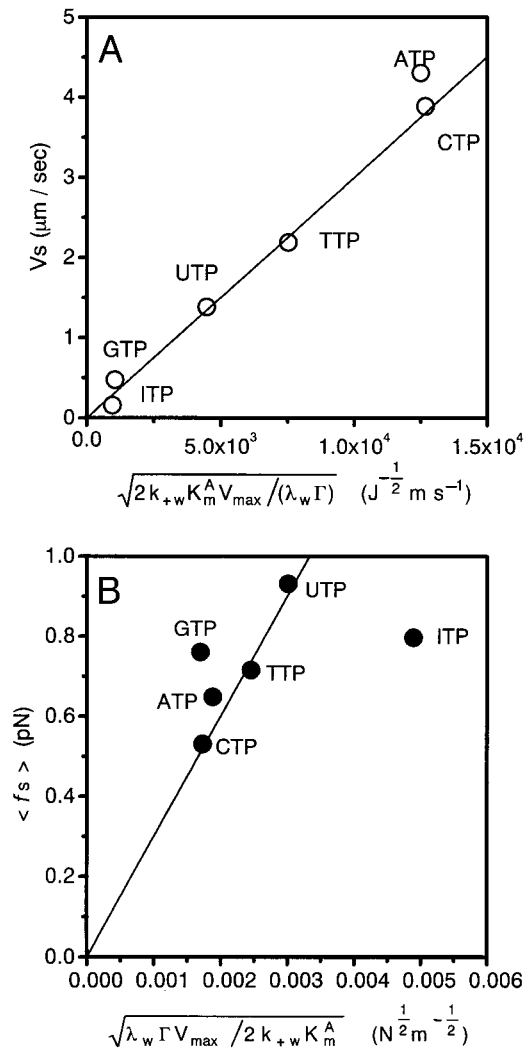
have to say that this efficient energy transduction does not mean that all the chemical energy is used to perform external mechanical work. Under no external load, a large part of the energy is used to deform actin-bound cross-bridges, and therefore eventually dissipates as heat.

Now we discuss the experimental results with various MeATPs. The sliding forces with MnATP and NiATP were similar to those with MgATP. This observation, as well as Eq. 19, predicts that the maximum sliding velocity should be proportional to the maximum hydrolysis rates of these substrates. This was not the case. The maximum sliding velocities with MnATP and NiATP were smaller than expected from their V_{max} values (closed circles in Fig. 2). This suggests that the energy liberation by hydrolysis of these substrates or the efficiency of energy transduction by acto-HMM with these substrates is smaller than those with MgATP. The former possibility is unlikely. The type of cation that is bound to ATP should not strongly affect the extent of energy liberation, because there exist several enzymes that utilize CaATP, Na-ATP, or K-ATP as energy sources. Equation 7 predicts that the maximum sliding velocity, V_s^{max}, should be proportional to $k_{+w}K_m^A/\lambda_w$. The value of V_s^{max} with NiATP was smaller than expected from the K_m^A value (Fig. 3). This is understandable because k_{+w}/λ_w with NiATP is smaller than those with MgATP and MnATP (see Table 3). Since the values of V_{max}/K_m^A for MgATP and NiATP (0.8×10^6 M^{-1} s^{-1} and 0.9×10^6 M^{-1} s^{-1}, respectively) are quite similar, the smaller pd and k_{+w}/λ_w cancel out to afford NiATP $\langle f_s \rangle$ similar to that with MgATP (see Eq. 21).

Relevance to other studies

It has been studied how noncycling unphosphorylated smooth muscle or nonmuscle myosin affects the actin sliding produced by cycling myosins (Warshaw et al., 1990; Cuda et al., 1997). These noncycling myosins weakly bind to actin. The sliding velocity generated by phosphorylated smooth muscle myosin was only slightly reduced by unphosphorylated smooth muscle myosin. For instance, when the mixing ratio (r) of unphosphorylated myosin over phosphorylated myosin was 1, the reduction rate was ~20%. A similar small reduction was also observed in the mixture of phosphorylated platelet and unphosphorylated platelet myosin. These small reductions apparently imply that weakly bound cross-bridges generate little resistive force. According to our force-balance model, a main determinant for the reduction in this mixing assay is the ratio of the dissociation rate constant (k_{-w}) of cycling myosin in the weak-binding states over that of unphosphorylated species (k_{-w}^u), i.e., $V_s = V_s^{max}/(1 + rk_{-w}/(\lambda_w k_{-w}^u))$. The larger ratio ($k_{-w}/k_{-w}^u$) will give a greater reduction in the actin filament velocity. Under an assumption, $\lambda_w = 0.8$, analysis of the data (Figs. 8 and 9 of Cuda et al., 1997) based on this model predicts that k_{-w}^u is ~5 times larger than k_{-w} of corresponding

FIGURE 6 The relationships (a) between V_s^{max} vs. $\sqrt{2k_{+w}K_m^A V_{max}/(\lambda_w \Gamma)}$ ($\bigcirc$) and (b) between $\langle f_s \rangle$ vs. $\sqrt{\lambda_w \Gamma V_{max}/(2k_{+w}K_m^A)}$ ($\bullet$).

phosphorylated myosin in the weak-binding states. This prediction may come true, because in ATP unphosphorylated smooth muscle myosin has 4–10-times lower actin affinity than its phosphorylated form (Ikebe et al., 1981; Sellers et al., 1982). When unphosphorylated platelet myosin was mixed with skeletal muscle myosin, the reduction rate was approximately proportional to the mixing ratio (Cuda et al., 1997). This suggests, according to our force-balance model, that the dissociation rate of unphosphorylated platelet myosin is similar to that of skeletal muscle myosin in the weak-binding states (i.e., $k_{-w}^u \simeq k_{-w}$). Pairwise mixings of different types of actively cycling myosins revealed that only small proportions of a more slowly translating myosin type significantly inhibited the sliding velocity generated by a more rapidly translocating myosin type (Warshaw et al., 1990; Cuda et al., 1997). The dissociation rate of weakly bound cross-bridges probably differs greatly between the two myosin types, so a large inhibition of actin sliding is expected to be caused by the slower myosin type. In addition to this, the cross-bridges that are slowly executing the power strokes in the strong-binding states (the power-stroke time, T_p^{slow}) also produce resistive forces against the actin filaments that are sliding at V_s larger than the power-stroke speed, d/T_p^{slow}.

Myosin heads with ATPγS weakly attach to actin (the hydrolysis rate is negligibly small). The actin sliding velocity in the presence of 1 mM ATP + 5 mM ATPγS is ~80% of that in 1 mM ATP without ATPγS (Homsher et al., 1992), apparently implying that weakly attached cross-bridges do not play a predominant role in limiting the rate of movement. However, in this report there are not presented experimental data as to the fraction of actin-attached myosin heads that are occupied with ATPγS, so we measured the acto-HMM ATPase activity in the presence of 1 mM ATP and various concentrations (0–5 mM) of ATPγS (data not shown). The ATPase activity was little inhibited (5% at most) even by 5 mM ATPγS, indicating a very low affinity of ATPγS for acto-HMM compared with ATP, coinciding with Goody and Hofmann (1980).

In addition to k_{-w} and the rate constant of the rate-limiting step, the elasticity of actin-attached cross-bridges seems an important factor in determining the mechanical behavior of actomyosin. The more stiff cross-bridges result in slower sliding movement and higher force generation, as indicated by Eqs. 20 and 21. This effect may account, in part, for variation of the rate of movement among different myosin species, and also possibly among different actin species that have different structures at the myosin binding sites. A series of mutant *Dictyostelium* myosins that have different neck lengths propel movement of actin filaments at distinct velocities. The velocity increases with increasing neck length (Uyeda et al., 1996). Although this behavior has been interpreted by the "swinging lever arm model," it can be accounted for by differences in the elasticity of the neck region that depends on length.

We surveyed previous studies that have compared the rates of actin translocation with the ATPase activities using various myosin species, actin species, chemically modified actins, tropomyosin, or different solution conditions. A number of papers have reported complete sets of data for V_{max}, K_m^A, and V_s^{max}. Almost all the works have, however, measured V_s^{max} and (V_{max}, K_m^A) under different solution conditions. Nevertheless, we did analyze, using Eq. 20, the data that appeared in seven reports (Cook et al., 1993; Umemoto and Sellers, 1990; Sutoh et al., 1991; Johara et al., 1993; Crosbie et al., 1994; Rovner et al., 1995; Hozumi et al., 1996). The results are shown in Fig. 7, where the values of V_s^{max} and $\sqrt{V_{max}K_m^A}$ are normalized to the corresponding control values. Although scattered in a somewhat wide range, the plots are distributed around the diagonal straight line connecting the coordinates (0,0) and (1.8,1.8). This strongly suggests that V_s^{max} is approximately proportional to $\sqrt{V_{max}K_m^A}$. Johara et al. (1993) produced a mutant of *Dictyostelium* actin, and measured V_{max}, K_m^A, and active force generated by a single actin filament and rabbit skeletal HMM. The force and $\sqrt{V_{max}/K_m^A}$ with the mutant actin are 0.84 and 0.7, respectively, when normalized to those with the wild actin. This supports the proportional relationship between active force and $\sqrt{V_{max}/K_m^A}$.
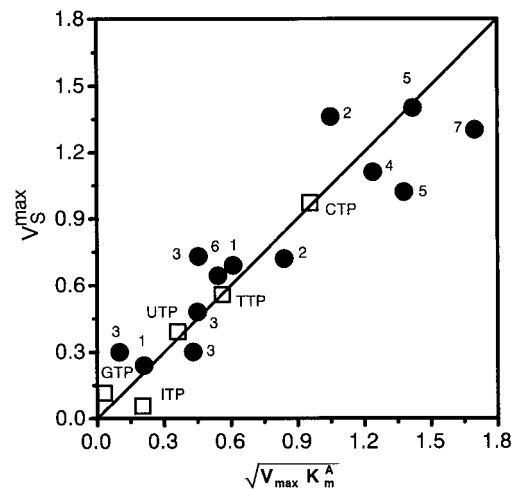

FIGURE 7   The relationship between V_s^{max} vs. $\sqrt{V_{max}K_m^A}$. The values of V_s^{max}, V_{max}, and K_m^A were quoted from seven published sources that have compared the rate of actin translocation with the ATPase activities using various myosin species, actin species, chemically modified actins, or tropomyosin (●). The values of V_s^{max} and $\sqrt{V_{max}K_m^A}$ were normalized to the corresponding control values. The numbers attached to each data point represent the literature quoted here. (1) *Dictyostelium* actin mutants (Sutoh et al., 1991). (2) Chemically modified actins (Crosbie et al., 1994). (3) 50K/20K loop-substituted smooth muscle HMMs (Rovner et al., 1995). (4) Yeast myosin mutant (Cook et al., 1993). (5) Mono and diphosphorylated smooth muscle HMMs and effect of tropomyosin (Umemoto et al., 1989). (6) Chemically modified actin (Hozumi et al., 1996). (7) *Dictyostelium* actin mutant (Johara et al., 1993). The values of V_s^{max}, V_{max}, and K_m^A are those obtained in the present study with various MgNTPs (□). The values of V_s^{max} and $\sqrt{V_{max}K_m^A}$ were normalized to the corresponding values for MgATP.

In this report we showed that the resistive force produced by weakly bound cross-bridges plays an important role in determining the sliding velocity. We considered only a situation where actin filaments are sliding on HMM without external load or under small external load. Within this limitation, Eqs. 20 and 21 can be fundamental equations that link the mechanical behaviors of skeletal actomyosin to the enzymatic kinetics. However, for different types of myosins whose kinetic mechanisms are largely different from that of skeletal myosin, these equations have to be modified.

REFERENCES

Ando, T. 1984. Fluorescence of fluorescein attached to myosin SH1 distinguishes the rigor state from the actin-myosin-nucleotide state. *Biochemistry.* 23:375–381.

Arheden, H., A. Arner, and P. Hellstrand. 1988. Cross-bridge behavior in skinned smooth muscle of the guinea-pig taenia coli at altered ionic strength. *J. Physiol.* 403:539–558.

Bárány, M. 1967. ATPase activity of myosin correlated with speed of muscle shortening. *J. Gen. Physiol.* 50:197–216.

Barman, T., M. Brune, C. Lionne, N. Piroddi, C. Poggesi, R. Stehle, C. Tesi, F. Travers, and M. R. Webb. 1998. ATPase and shortening rates in frog fast skeletal myofibrils by time-resolved measurements of protein-bound and free Pi. *Biophys. J.* 74:3120–3130.

Bell, G. I. 1978. Models for the specific adhesion of cells to cells. *Science.* 200:618–627.

Blum, J. J. 1955. The enzymatic interaction between myosin and nucleotides. *Arch. Biochem. Biophys.* 55:486–511.

Bobkov, A. A., E. A. Bobkov, S.-H. Lin, and E. Reisler. 1996. The role of surface loop (residues 204–216 and 627–646) in the motor function of the myosin head. *Proc. Natl. Acad. Sci. USA.* 93:2285–2289.

Borejdo, J., T. Ando, and T. P. Burghardt. 1985. The rate of MgADP binding to and dissociation from acto-S1. *Biochim. Biophys. Acta.* 828:172–176.

Brenner, B. 1990. Muscle mechanics and biochemical kinetics. *In* Molecular Mechanisms in Muscular Contraction. J. M. Squire, editor. Macmillan Press, London. 77–149.

Brune, M., J. L. Hunter, J. E. T. Corrie, and M. R. Webb. 1994. Direct, real-time measurement of rapid inorganic phosphate release using a novel fluorescent probe and its application to actomyosin subfragment 1. *Biochemistry.* 33:8262–8271.

Cook, R. K., D. Root, C. Miller, E. Reisler, and P. A. Rubenstein. 1993. Enhanced stimulation of myosin subfragment 1 ATPase activity by addition of negatively charged residues to the yeast actin NH$_2$ terminus. *J. Biol. Chem.* 268:2410–2415.

Cooke, R. 1995. The actomyosin engine. *FASEB J.* 9:636–642.

Cooke, R. 1997. Actomyosin interaction in striated muscle. *Physiol. Rev.* 77:671–697.

Cooke, R., and W. Bialek. 1979. Contraction of glycerinated muscle fibers as a function of the ATP concentration. *Biophys. J.* 28:241–258.

Crosbie, R. H., C. Miller, P. Cheung, T. Goodnight, A. Muhlrad, and E. Reisler. 1994. Structural connectivity in actin: effect of C-terminal modifications on the properties of actin. *Biophys. J.* 67:1957–1964.

Cuda, G., E. Pate, R. Cooke, and J. R. Sellers. 1997. In vitro actin filament sliding velocities produced by mixtures of different types of myosin. *Biophys. J.* 72:1767–1779.

Dantzig, J. A., Y. E. Goldman, N. C. Millar, J. Lacktis, and E. Homsher. 1992. Reversal of the cross-bridge force-generating transition by photogeneration of phosphate in rabbit psoas muscle fibers. *J. Physiol.* 451:247–278.

DiSanto, M. E., R. H. Cox, Z. Wang, and S. Chacko. 1997. NH$_2$-terminal-inserted myosin II heavy chain is expressed in smooth muscle of small muscular arteries. *Am. J. Physiol. Cell Physiol.* 272:C1532–C1542.

Eccleston, J. F., and D. R. Trentham. 1979. Magnesium ion dependent rabbit skeletal muscle myosin guanosine and thioguanosine triphosphatase mechanism and a novel guanosine diphosphatase reaction. *Biochemistry.* 18:2896–2904.

Edman, K. A. P., C. Reggiani, S. Schiaffino, and G. T. E. Kronnie. 1988. Maximum velocity of shortening related to myosin isoform composition in frog skeletal muscle fibers. *J. Physiol.* 395:679–694.

Ferenczi, M. A., Y. E. Goldman, and R. M. Simmons. 1984. The dependence of force and shortening velocity on substrate concentration and skinned fibers from frog muscle. *J. Physiol.* 350:519–543.

Fiske, C. H., and Y. Subbarow. 1925. The colorimetric determination of phosphorus. *J. Biol. Chem.* 14:1–10.

Galler, S., and W. Rathmayer. 1992. Shortening velocity and force/pCa relationship in skinned crab muscle fibers of different types. *Pflügers Arch.* 420:187–193.

Goody, R. S., and W. Hofmann. 1980. Stereochemical aspects of the interaction of myosin and actomyosin with nucleotides. *J. Muscle Res. Cell Motil.* 1:101–115.

Gulati, J., and R. J. Podolsky. 1981. Isotonic contraction of skinned muscle fibers on a slow time base. *J. Gen. Physiol.* 78:233–257.

Haeberle, J. R. 1994. Calponin decreases the rate of cross-bridge cycling and increases maximum force production by smooth muscle myosin in an in vitro motility assay. *J. Biol. Chem.* 269:12424–12431.

Harada, Y., A. Noguchi, A. Kishino, and T. Yanagida. 1987. Sliding movement of single actin filaments on one-headed myosin filaments. *Nature.* 326:805–808.

Hasselbach, W. 1956. Die Wechselwirkung verchiedener Nukleosidtriphosphate mit Aktomyosin im Gelzustand. *Biochim. Biophys. Acta.* 20:355–368.

He, Z.-H., R. K. Chillingworth, M. Brune, J. E. T. Corrie, D. R. Trentham, M. R. Webb, and M. A. Ferenczi. 1997. ATPase kinetics on activation of rabbit and frog permeabilized isometric muscle fibers: a real time phosphate assay. *J. Physiol.* 501:125–148.

He, Z.-H., G. J. M. Stienen, J. P. F. Barends, and M. A. Ferenczi. 1998. Rate of phosphate release after photoliberation of adenosine 5′-triphosphate in slow and fast muscle fibers. *Biophys. J.* 75:2389–2401.

Helper, D. J., J. A. Lash, and D. R. Hathaway. 1988. Distribution of isoelectric variants of the 17,000-dalton myosin light chain in mammalian smooth muscle. *J. Biol. Chem.* 263:15748–15753.

Hibberd, M. G., and D. R. Trentham. 1986. Relationships between chemical and mechanical events during muscle contraction. *Annu. Rev. Biophys. Biophys. Chem.* 15:119–161.

Higashi-Fujime, S. 1991. Reconstitution of active movement in vitro based on the actin-myosin interaction. *Int. Rev. Cytol.* 125:95–138.

Higashi-Fujime, S., and T. Hozumi. 1996. The mechanism for mechanochemical energy transduction in actin-myosin interaction revealed by in vitro motility assay with ATP analogues. *Biochem. Biophys. Res. Commun.* 221:773–778.

Homsher, E., F. Wang, and J. R. Sellers. 1992. Factors affecting movement of F-actin filaments propelled by skeletal muscle heavy meromyosin. *Am. J. Physiol. Cell Physiol.* 262:C714–C723.

Hozumi, T., M. Miki, and S. Higashi-Fujime. 1996. Maleimidobenzoyl actin: its biochemical properties and in vitro motility. *J. Biochem.* 119:151–156.

Huxley, A. F. 1957. Muscle structure and theories of contraction. *Prog. Biophys. Biophys. Chem.* 7:255–318.

Ikebe, M., Y. Tonomura, H. Onishi, and S. Watanabe. 1981. Elementary steps in the F-actin activated Mg^{2+}-ATPase reaction of gizzard

h-meromyosin: effects of phosphorylation of the light-chain subunit. *J. Biochem.* 90:61–77.

Ishijima, A., T. Doi, K. Sakurada, and T. Yanagida. 1991. Subpiconewton force fluctuations of actomyosin in vitro. *Nature.* 352:301–306.

Ishijima, A., H. Kojima, H. Higuchi, Y. Harada, T. Funatsu, and T. Yanagida. 1996. Multiple- and single-molecule analysis of the actomyosin motor by nanometer-piconewton manipulation with a microneedle: unitary steps and force. *Biophys. J.* 70:383–400.

Johara, M., Y. Y. Toyoshima, A. Ishijima, H. Kojima, T. Yanadida, and K. Sutoh. 1993. Charge-reversion mutagenesis of *Dictyostelium* actin to map the surface recognized by myosin during ATP-driven sliding motion. *Proc. Natl. Acad. Sci. USA.* 90:2127–2131.

Kim, E., C. J. Miller, and E. Reisler. 1996. Polymerization and in vitro motility properties of yeast actin: a comparison with rabbit skeletal α-actin. *Biochemistry.* 35:16566–16572.

Kron, S. J., and J. A. Spudich. 1986. Fluorescent actin filaments move on myosin fixed to a glass surface. *Proc. Natl. Acad. Sci. USA.* 83: 6272–6276.

Lowey, S., G. S. Waller, and K. M. Trybus. 1993. Function of skeletal muscle myosin heavy and light chain isoforms by an in vitro motility assay. *J. Biol. Chem.* 268:20414–20418.

Lund, J., M. R. Webb, and D. C. S. White. 1987. Changes in the ATPase mechanism of insect fibrillar flight muscle during Ca^{2+} and strain activation probed by phosphate-water oxygen exchange. *J. Biol. Chem.* 262:8584–8590.

Malmqvist, U., and A. Arner. 1991. Correlation between isoform composition of the 17 kDa myosin light chain and maximum shortening velocity in smooth muscle. *Pflügers Arch.* 418:523–530.

Mehta, A. D., J. T. Finer, and J. A. Spudich. 1997. Detection of single-molecule interactions using correlated thermal diffusion. *Proc. Natl. Acad. Sci. USA.* 94:7927–7931.

Miller, C. J., W. W. Wong, E. Bobkova, P. A. Rubenstein, and E. Reisler. 1996. Mutational analysis of the role of the N terminus of actin in actomyosin interactions. Comparison with other mutant actins and implications for the cross-bridge cycle. *Biochemistry.* 35:16557–16565.

Murphy, C. T., and J. A. Spudich. 1998. *Dictyostelium* myosin 20–50K loop substitutions specifically affect ADP release rates. *Biochemistry.* 37:6738–6744.

Nakajima, H., Y. Kunioka, K. Nakano, K. Shimizu, M. Seto, and T. Ando. 1997. Scanning force microscopy of the interaction events between a single molecule of heavy meromyosin and actin. *Biochem. Biophys. Res. Commun.* 234:178–182.

Nishizaka, T., H. Miyata, H. Yoshikawa, S. Ishiwata, and K. Kinoshita, Jr. 1995. Unbinding force of a single motor molecule of muscle measured using optical tweezers. *Nature.* 377:251–254.

Okagaki, T., S. Higashi-Fujime, R. Ishikawa, H. Takano-Ohmuro, and K. Kohama. 1991. In vitro movement of actin filaments on gizzard smooth muscle myosin: requirement of phosphorylation of myosin light chain and effects of tropomyosin and caldesmon. *J. Biochem.* 109:858–866.

Pate, E., K. Franks-Skiba, H. White, and R. Cooke. 1993. The use of differing nucleotides to investigate cross-bridge kinetics. *J. Biol. Chem.* 268:10046–10053.

Regnier, M., D. M. Lee, and E. Homsher. 1998. ATP analogs and muscle contraction: mechanics and kinetics of nucleotide triphosphate binding and hydrolysis. *Biophys. J.* 74:3044–3058.

Rosenfeld, S. S., and E. W. Taylor. 1984. The ATPase mechanism of skeletal and smooth muscle acto-subfragment 1. *J. Biol. Chem.* 259: 11908–11919.

Rovner, A. S., Y. Freyzon, and K. M. Trybus. 1995. Chimeric substitutions of the actin-binding loop activate dephosphorylated but not phosphorylated smooth muscle heavy meromyosin. *J. Biol. Chem.* 270: 30260–30263.

Saito, K., T. Aoki, T. Aoki, and T. Yanagida. 1994. Movement of single myosin filaments and myosin step size on an actin filament suspended in solution by a laser trap. *Biophys. J.* 66:769–777.

Schwyter, D. H., S. J. Kron, Y. Y. Toyoshima, J. A. Spudich, and E. Reisler. 1990. Subtilisin cleavage of actin inhibits in vitro sliding movement of actin filaments over myosin. *J. Cell Biol.* 111:465–470.

Sellers, J. R., E. Eisenberg, and R. S. Adelstein. 1982. The binding of smooth muscle heavy meromyosin to actin in the presence of ATP. *J. Biol. Chem.* 257:13880–13883.

Sheetz, M. P., R. Chasan, and J. A. Spudich. 1984. ATP-dependent movement of myosin in vitro: characterization of a quantitative assay. *J. Cell Biol.* 99:1867–1871.

Sheetz, M. P., and J. A. Spudich. 1983. Movement of myosin-coated fluorescent beads on actin cables in vitro. *Nature.* 303:31–35.

Shimizu, T., K. Furusawa, S. Ohashi, Y. Y. Toyoshima, M. Okuno, F. Malik, and R. D. Vale. 1991. Nucleotide specificity of the enzymatic and motile activities of dynein, kinesin, and heavy meromyosin. *J. Cell Biol.* 112:1189–1197.

Siemankowski, R. F., M. O. Wiseman, and H. D. White. 1985. ADP dissociation from actomyosin subfragment 1 is sufficiently slow to limit the unloaded shortening velocity in vertebrate muscle. *Proc. Natl. Acad. Sci. USA.* 82:658–662.

Sleep, J. A., and R. L. Hutton. 1980. Exchange between inorganic phosphate and adenosine 5′-triphosphate in the medium by actomyosin subfragment 1. *Biochemistry.* 19:1276–1283.

Spudich, J. A., and S. Watt. 1971. The regulation of rabbit skeletal muscle contraction. I. Biochemical studies of the tropomyosin-troponin complex with actin and the proteolytic fragments of myosin. *J. Biol. Chem.* 246:4866–4871.

Stein, L. A., P. B. Chock, and E. Eisenberg. 1984. The rate-limiting step in the actomyosin adenosine triphosphatase cycle. *Biochemistry.* 23: 1555–1563.

Stein, L. A., R. P. Schwarz, P. B. Chock, and E. Eisenberg. 1979. Mechanism of actomyosin adenosine triphosphatase. Evidence that adenosine 5′-triphosphate hydrolysis can occur without dissociation of the actomyosin complex. *Biochemistry.* 18:3895–3909.

Stone, D. B., and S. C. Prevost. 1973. Characterization of modified myosin at low ionic strength. Enzymatic and spin-label studies. *Biochemistry.* 12:4206–4211.

Stryer, L. 1981. Biochemistry, 2nd Ed. W. H. Freeman and Company, San Francisco.

Sugiura, S., H. Yamashita, T. Serizawa, M. Iizuka, T. Shimmen, and T. Sugimoto. 1992. Active movement of cardiac myosin on Characeae actin cables. *Pflügers Arch.* 421:32–36.

Sutoh, K., M. Ando, K. Sutoh, and Y. Yano-Toyoshima. 1991. Site-directed mutations of *Dictyostelium* actin: disruption of a negative charge cluster at the N terminus. *Proc. Natl. Acad. Sci. USA.* 88: 7711–7714.

Takiguchi, K., H. Hayashi, E. Kurimoto, and S. Higashi-Fujime. 1990. In vitro motility of skeletal muscle myosin and its proteolytic fragments. *J. Biochem.* 107:671–679.

Tawada, K., and K. Sekimoto. 1991. A physical model of ATP-induced actin-myosin movement in vitro. *Biophys. J.* 59:343–356.

Tonomura, Y., P. Appel, and M. F. Morales. 1966. On the molecular weight of myosin. *Biochemistry.* 5:515–521.

Toyoshima, Y. Y., S. J. Kron, E. M. McNally, K. R. Niebling, C. Toyoshima, and J. A. Spudich. 1987. Myosin subfragment-1 is sufficient to move actin filaments in vitro. *Nature.* 328:536–539.

Umemoto, S., A. R. Bengur, and J. R. Sellers. 1989. Effect of multiple phosphorylations of smooth muscle and cytoplasmic myosins on movement in an in vitro motility assay. *J. Biol. Chem.* 264:1431–1436.

Umemoto, S., and J. R. Sellers. 1990. Characterization of in vitro motility assays using smooth muscle and cytoplasmic myosins. *J. Biol. Chem.* 265:14864–14869.

Uyeda, T. Q. P., P. D. Abramson, and J. A. Spudich. 1996. The neck region of the myosin motor domain acts as a lever arm to generate movement. *Proc. Natl. Acad. Sci. USA.* 93:4459–4464.

Uyeda, T. Q. P., S. J. Kron, and J. A. Spudich. 1990. Myosin step size. Estimation from slow sliding movement of actin over low densities of heavy meromyosin. *J. Mol. Biol.* 214:699–710.

Uyeda, T. Q. P., K. M. Ruppel, and J. A. Spudich. 1994. Enzymatic activities correlate with chimeric substitutions at the actin-binding face of myosin. *Nature.* 368:567–569.

Uyeda, T. Q. P., H. M. Warrick, S. J. Kron, and J. A. Spudich. 1991. Quantized velocities at low densities in an in vitro motility assay. *Nature*. 352:307–311.

Vale, R. D., and F. Oosawa. 1990. Protein motors and Maxwell's demons: does mechanochemical transduction involve a thermal ratchet? *Adv. Biophys*. 26:97–134.

Vale, R. D., A. G. Szent-Györgyi, and M. P. Sheetz. 1984. Movement of scallop myosin on *Nitella* actin filaments: regulation by calcium. *Proc. Natl. Acad. Sci. USA*. 81:6775–6778.

Wahr, P. A., and J. M. Metzger. 1998. Peak power output is maintained in rabbit psoas and rat soleus single muscle fibers when CTP replaces ATP. *J. Appl. Physiol*. 85:76–83.

Wang, F., B. M. Martin, and J. R. Sellers. 1993. Regulation of actomyosin interactions in *Limulus* muscle proteins. *J. Biol. Chem*. 268:3776–3780.

Warshaw, D. M., J. M. Desrosiers, S. S. Work, and K. M. Trybus. 1990. Smooth muscle myosin cross-bridge interactions modulate actin filament sliding velocity in vitro. *J. Cell Biol*. 111:453–463.

Webb, M. R., and D. R. Trentham. 1981. The mechanism of ATP hydrolysis catalyzed by myosin and actomyosin using rapid reaction techniques to study oxygen exchange. *J. Biol. Chem*. 256:10910–10916.

Weeds, A. G., and B. Pope. 1977. Studies on the chymotryptic digestion of myosin. Effect of divalent cations on proteolytic susceptibility. *J. Mol. Biol*. 111:129–157.

White, H. D., B. Belknap, and W. Jiang. 1993. Kinetics of binding and hydrolysis of a series of nucleotide triphosphates by actomyosin-S1. *J. Biol. Chem*. 268:10039–10045.

White, H. D., B. Belknap, and M. R. Webb. 1997. Kinetics of nucleotide triphosphate cleavage and phosphate release steps by associated rabbit skeletal actomyosin, measured using a novel fluorescent probe for phosphate. *Biochemistry*. 36:11828–11836.

White, H. D., and E. W. Taylor. 1976. Energetics and mechanism of actomysin adenosine triphosphatase. *Biochemistry*. 15:5818–5826.

Wolenski, J. S., R. E. Cheney, P. Forcher, and M. S. Mooseker. 1993. In vitro motilities of the unconventional myosins, brush border myosin-I, and chick brain myosin-V exhibit assay-dependent differences in velocity. *J. Exp. Zool*. 267:33–39.

Yanagida, T., M. Nakase, K. Nishiyama, and F. Oosawa. 1984. Direct observation of motion of single F-actin filaments in the presence of myosin. *Nature*. 307:58–60.